Department of Arctic and Marine Biology

Role of the lactate receptor HCAR1 as part of neural adaptations to hypoxia in hooded seals (*Cystophora cristata*)

Sara Torppa

Master's thesis in Biology BIO-3950 November 2023
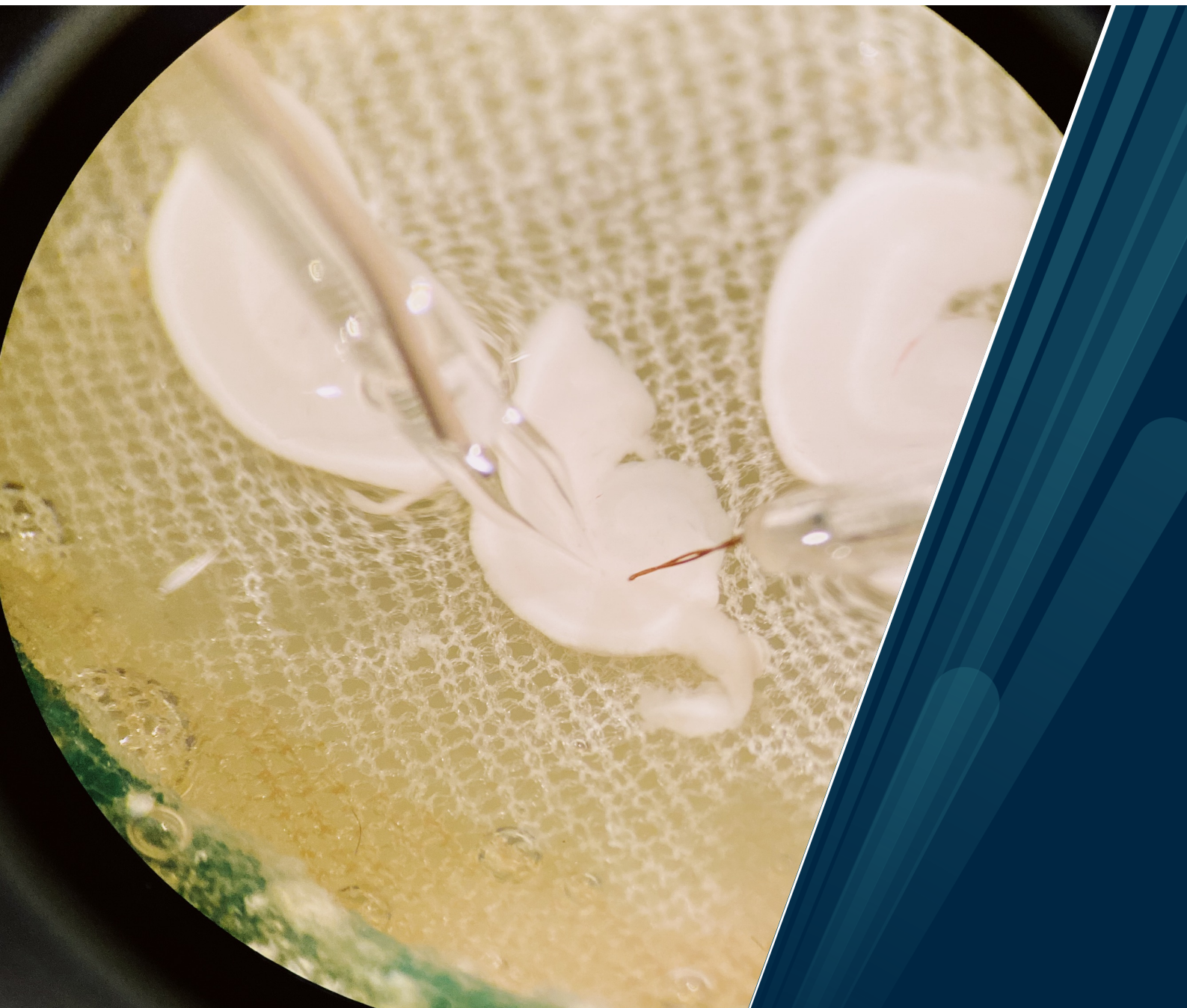
Cover photo by Torppa, S. K. (2023). The photograph shows a hippocampal slice taken from a hooded seal (*Cystophora cristata*), with a stimulating electrode (right) and a glass-recording electrode (left) placed to record field excitatory post-synaptic potentials (fEPSP) evoked by the stimulating electrode.

UiT The Arctic University of Norway

Faculty of Biosciences, Fisheries and Economics
Department of Arctic and Marine Biology

Role of lactate receptor HCAR1 as part of neural adaptations to hypoxia in hooded seals (*Cystophora cristata*)

Sara Torppa
Master of Science in Biology – Arctic Animal Physiology
November 2023

Main supervisor
Samuel Geiseler, UiT – The Arctic University of Norway
Co-supervisor
Lars Folkow, UiT – The Arctic University of Norway

Acknowledgements

First and foremost, I would like to express my gratitude to my two amazing supervisors, Samuel Geiseler and Lars Folkow, for their guidance and support during this project. Thank you for trusting me with it and providing me the opportunity to challenge myself. I feel lucky for having you both as my supervisors.

Samuel, thank you for teaching me so much about electrophysiology, and your incredible support during our lab experiments. Thank you for encouraging me to be more independent, and answering my questions, both silly and relevant.

Lars, thank you for your great guidance, input and support during this thesis and my studies. Thank you for welcoming me in the group already as an exchange student, it has made a great impact in my study path and life overall.

I would like to thank everyone who has helped me during the process of this project: Trine Lund for helping me with everything related to qPCR analysis. All the technicians for taking good care of the research animals and therefore making the research possible. Thank you everyone in the Arctic Chronobiology and Physiology group who has supported me during this time, especially Alexander West.

I also want to thank my friends and family for the support during these past years: I would not be here without you. Thank you everyone both from Tromsø and back home in Finland. Thank you Sari and Anna, for sharing the long days and nights in the lab and in the office! Special thanks go to my friend Emmi.

And, of course, thank you Matti for being my greatest support.

Last but not least, I want to thank my parents for all their support: Kiitos äiti ja isä!

Abstract

To maintain normal neuronal function, the mammalian brain requires a constant supply of energy. The deep-diving hooded seal (*Cystophora cristata*) brain exhibits remarkable tolerance to extreme hypoxia, presumably involving a reduction in brain activity to lower energy demand. Thus, some neurons, circuits or even regions in the seal's brain presumably display a neural protective shutdown response to achieve this. The mechanisms behind this response as yet remain incompletely understood, but there are several factors that may contribute.

Lactate, beyond its metabolic role, has been demonstrated to have signaling effects, and the lactate receptor HCAR1 is expressed in the human and rodent brain. Activation of HCAR1 has been observed to slow neuronal firing, inhibit excitatory transmission, and have other beneficial cerebral effects. This thesis investigates the role of the receptor in the hypoxia-tolerant hooded seal. Using qPCR analysis, the HCAR1 was shown to be expressed in several brain regions of hooded seals. Electrophysiological experiments, employing field recordings of excitatory post-synaptic potentials (fEPSP) were conducted to measure synaptic transmission in hippocampal slices from hooded seals. These recordings were performed with and without activating HCAR1 using lactate and non-metabolic agonists. Parallel experiments were conducted in mice to compare possible differences between hooded seals and non-hypoxia-tolerant animals. Both lactate and its agonist 3,5-DHBA demonstrated a suppressing effect on synaptic transmission activity in both hooded seals and mice. The results indicate that during the deep and prolonged dives of hooded seals, when energy is generated anaerobically in the brain, increased lactate levels activate HCAR1, leading to the suppression of synaptic activity. This mechanism potentially contributes to the neural protective shutdown observed in hooded seals.

Keywords: hooded seal (Cystophora cristata), lactate, HCAR1, hypoxia, brain, hippocampus, fEPSP, electrophysiology

Table of Contents

List of Tables

List of Figures

List of abbreviations

aCSF = artificial cerebrospinal fluid

AMPA = α-amino-3-hydroxy-5-methyl-4-isoxazolepropionic acid receptor

ANLS = astrocyte neuron lactate shuttle

ATP = adenosine triphosphate

cDNA = complementary deoxyribonucleic acid

CNS = central nervous system

fEPSP = field excitatory post synaptic potential

GPCRs = G-protein coupled receptors

HCAR1 = hydroxycarboxylic acid receptor 1

KO = knockout

NMDA = N-methyl-D-aspartate receptor

mRNA = messenger RNA

PPF = paired pulse facilitation

ROS = reactive oxygen species

RT-qPCR = reverse transcription quantitative polymerase chain reaction

WT = wild-type

1 Introduction

1.1 Mammalian brain and its energy requirements

The mammalian brain is known to be vulnerable to lack of oxygen due to its large oxygen consumption. In the case of humans, the brain represents only 2% of the body mass, but consumes approximately 20% of the body's total oxygen supply (Mink et al., 1981; Rolfe and Brown, 1997). This heightened oxygen demand is primarily due to the brain's composition of neurons, which communicate continuously through action potentials and synaptic transmission. To enable sufficient function of the complex signaling mechanisms, efficient energy supply is needed since most of the brain's energy supply (adenosine triphosphate, ATP) is used to maintain the membrane potential during synaptic transmission (Harris et al., 2012). Cardiovascular diseases and events like stroke, often cause reduced bloodflow to the brain (ischemia) leading to insufficient oxygen supply (hypoxia), causing detrimental effects (Dirnagl et al., 1999). Extensive research has been dedicated to understanding the pathophysiology ischemia/hypoxia, but despite this, cardiovascular diseases such as stroke persist as one of the leading causes of human death in the Western world (Tsao et al., 2023).

1.2 Neural activity requires constant energy supply to the brain

The primary mechanism behind the production of ATP is mitochondrial oxidative phosphorylation, which also explains the high cerebral dependency on oxygen. For oxidative phosphorylation to occur and therefore generate sufficient levels of ATP, a constant supply of oxygen is needed. The main metabolic fuel for most organs is glucose, and energy is liberated from it through two consecutive processes: glycolysis in the cytosol, and oxidative phosphorylation in mitochondria (Erecinska and Silver, 1989). Under normoxic conditions, more than 95 % of the brain ATP is generated via oxidative phosphorylation – one mole of glucose yields 36 moles of ATP. Thus, it yields 17-18 times more energy than anaerobic glycolysis, that produces 2 moles of ATP per one mol of glucose (Erecinska and Silver, 1994).

Most of the produced ATP required for adequate neural function in the brain is used for ion pumping needed to maintain different concentrations of the ions (Na^+, K^+, Ca^{2+}, Cl^-) across

the membrane of neurons. This creates an electrochemical gradient over the neuronal plasma membrane, referred as the resting membrane potential (Erecinska and Silver, 1994; Larson et al., 2014). The gradient across the membrane is maintained by transmembrane proteins, known as ion pumps, that use ATP to transport ions from low concentration to high concentration, against their concentration gradient. The most important ion pump in this context is Na^+/K^+-ATPase, which transfers 3 sodium ions out and 2 potassium ions into the cell per each ATP molecule it consumes (Erecinska and Silver, 2001; Lutz et al., 2003). Without this energy-consuming ion pumping to maintain the resting membrane potential, normal cerebral functions such as generation and transmission of impulses cannot be accomplished (Lipton 1999). While action potentials result in a rapid increase of positive intracellular ions via the opening of voltage gated Na^+ channels, the overall bulk flow of these ions is minimal. This indicates that the energy spent to reestablish the disrupted ion balance due to action potentials is relatively minor (Alle et al., 2009), and the main energy consumption in neurons takes place in the synapses (Harris et al., 2012).

In chemical synapses, synaptic transmission begins with the arrival of an action potential to the axon terminal of the presynaptic neuron, triggering the opening of voltage-gated Ca^{2+} channels. The axon terminal contains neurotransmitter molecules, such as glutamate, stored in synaptic vesicles. When Ca^{2+} ions enter the axon terminal, they stimulate the fusion of vesicles with the presynaptic membrane, leading to the release of neurotransmitters through exocytosis. These neurotransmitters then diffuse across the synaptic cleft and bind to postsynaptic receptors that are embedded in the postsynaptic membrane (Hill et al., 2018). When a neurotransmitter binds to an ionotropic receptor, such as e.g. AMPA (α-amino-3-hydroxy-5-methyl-4-isoxazolepropionic acid receptor) or NMDA (N-methyl-D-aspartate receptor), which are glutamate receptors, Na^{2+} ion channels open (Madden, 2002). This action creates an ionic current that alters the membrane potential of the postsynaptic cell, leading to postsynaptic depolarization. Signal transmission through this form is rapid, but there are also slower-working metabotropic G-protein coupled receptors (GPCRs). When neurotransmitters bind to GPCRs, they activate G proteins, leading to the production of second messengers such as cyclic AMP (cAMP) (Hill et al., 2018).

Restoring ion concentrations in the postsynaptic neuron following the transmission of the synaptic signals consumes a substantial amount of the energy used for synaptic transmission. Additionally, within the presynaptic terminal, maintaining ion balance and recycling neurotransmitter vesicles are processes that further contribute to the energy consumption

(Harris et al., 2012). ATP-dependent synaptic vehicle refilling is fueled by glycolysis (Ikemoto et al., 2003; Ishida et al., 2009) and inhibition of presynaptic glycolysis impairs synaptic vesicle packaging and recycling (Rangaraju et al., 2014) and therefore neurotransmission. However, most of the ATP consumption in synaptic transmission is used on reversing the ion movements that are responsible for generating postsynaptic responses in excitatory synapses (Harris et al., 2012).

Out of all the forms of energy substrate, blood glucose is the main fuel for the mammalian brain (Clarke and Sokoloff, 1999) and it can be metabolized to lactate in astrocytes. According to the astrocyte-neuron-lactate shuttle (ANLS) hypothesis, glutamate uptake into astrocytes stimulates glycolysis and lactate production to meet the energy needs of neurons. Astrocytes then supply neurons with lactate, to there being metabolized to pyruvate and further on via aerobic metabolism, to maximize the ATP yield (Pellerin & Magistretti, 1994; Bergersen 2007; Pellerin & Magistretti, 2012). Research also suggests an important role of ketone bodies as an energy fuel for the brain at times of glucose shortage, such as prolonged fasting (Sokoloff 1973; Morris 2005). In astrocytes, energy substrate can also be stored as glycogen and later be mobilized and subsequently metabolized to pyruvate (Brown and Ransom, 2007).

1.3 Hypoxia

Hypoxia is a state characterized by insufficient oxygen supply to tissues or organs. In cases of brain ischemia, the loss of blood supply results in a reduction of critical substrates, notably glucose and oxygen, to levels that are inadequate for sustaining normal function of the neural system (Dirnagl et al., 1999; Lipton 1999).

In the absence of oxidative phosphorylation, essential ATP-dependent neuronal processes including ion transport and re-uptake of neurotransmitters will decline rapidly, triggering excitotoxic cascade (**Figure 1**). When ATP -levels decrease, the Na^+/K^+-ATPase ion-pump will eventually reach a point where it will no longer be able to sustain the ion balance. Without ion-pumping, ion gradients will fail and cause depolarization of neurons, releasing excessive amounts of neurotransmitters including the excitatory neurotransmitter glutamate. Glutamate overstimulates and activates NMDA and AMPA receptors (Choi 1988; Novelli et al., 1988). This continuous excitation will cause an uncontrolled flood of Ca^{2+} both from

intra- and extracellular stores, leading to Ca^{2+} overload in the neurons (Lipton and Whittingham, 1979; Lipton 1999; Lutz et al., 2003). As an intracellular messenger, Ca^{2+} will subsequently over-activate several enzyme systems, resulting in generation of reactive oxygen species (ROS). These free radicals will damage cell membranes, mitochondria, and DNA, ultimately leading to trigger apoptosis (Dirnagl et al., 1999).
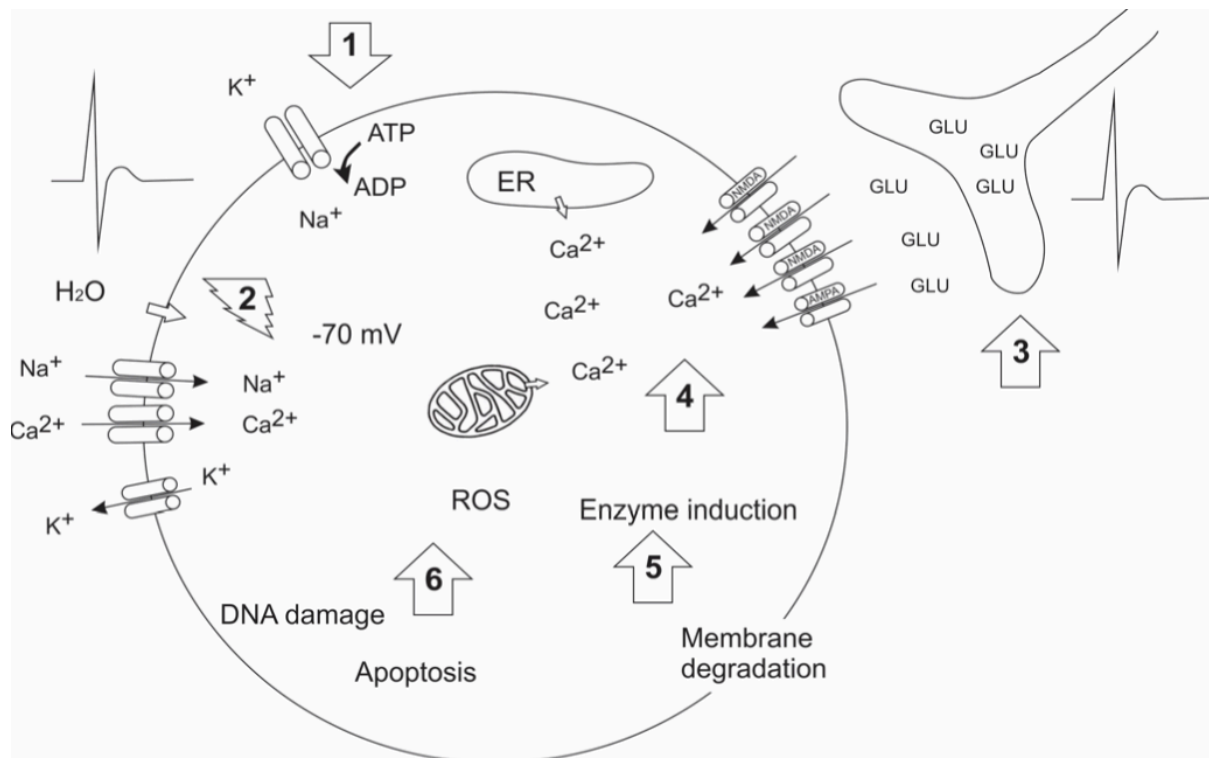
Figure 1 Excitotoxic cascade resulting from hypoxia. *1)* Energy failure. *2)* Depolarization due to disruption in ion balance. *3)* Uncontrolled release of glutamate resulting in over activation of NMDA and AMPA receptors. *4)* Ca^{2+} overload. *5)* Production of free radicals due to overactivation of enzyme systems. *6)* Damage in cell components and DNA, leading to apoptosis. ER = endoplasmic reticulum, ROS = radical oxygen species, GLU = glutamate. From Geiseler (2016), modified after Dirnagl et al. (1999) and Drew et al. (2004).

"*For a large number of problems there will be some animal of choice, or a few such animals, on which it can be most conveniently studied.*" - August Krogh, 1929.

Hypoxia can be detrimental for mammals, including humans, that are typically not adapted to tolerate it. However, there are animals with intrinsic adaptations to hypoxia that are capable to prevent excitotoxic cascade from happening (e.g., Larson et al., 2014). Diving mammals serve as a great example of a model animal when it comes to the research on finding mechanisms to prevent hypoxic damage – they may help us to understand how evolution through natural

selection has found solutions to the challenges associated with hypoxia. The hooded seal (*Cystophora cristata*) may serve as a suitable model for this purpose because of its deep-diving behavior (Folkow and Blix, 1995).

1.4 Hooded seal as a model animal

The hooded seal is a large pinniped species, belonging to the true seal family. They are named after the inflatable nasal septum of the male seals, which they use both to display territorial aggression towards other males but also to attract females (Kovacs and Lavigne, 1986; Blix, 2005). Hooded seals are distributed throughout the central and western North Atlantic Ocean, and their two main breeding stocks are reportedly located in east of Newfoundland, and between east coast of Greenland and Jan Mayen (Kovacs and Lavigne, 1986; Folkow et al., 1996). They are highly precocial animals with lactation period that lasts only 2-4 days. During this period pups gain weight fast from the extremely energy rich milk they feed on: they usually weight 25-30 kilograms when they are born, and after few days when they are weaned, they can weight up to 42 kilograms. Birth takes place between March and April on the ice (Bowen et al., 1985; Kovacs and Lavigne, 1986).

When it comes to diving behavior, hooded seals can be grouped in the deep-diving seals, together with species such as Weddell (*Leptonychotes weddelii*) and elephant seals (*Mirounga*). They undertake these deep dives to find and capture their food, mainly squid and fish. Hooded seals usually dive to 100–600-meter depths (Folkow & Blix, 1999), but dives deeper than 1000 meters have been recorded (Andersen et al., 2013; Vacquie-Garcia et al., 2017). Average diving durations are 13.5-14.5 minutes, but they have been recorded to perform more than 1-hour long dives (Folkow & Blix; Andersen et al., 2013).

1.4.1 General adaptations to diving

During the deep dives of hooded seals, they are not able to breath. To tolerate this issue, they are highly adapted with two main strategies: increased body oxygen reserves, and reduced oxygen demand in certain parts of the body. These strategies are supplemented with various defense and repair mechanisms to prevent, or diminish, hypoxic damage (Ramirez et al., 2007). Many animals lower their body metabolism to reduce their systemic energy demand, for instance during hibernation (Larson et al., 2014). A systemic shutdown, similar to that

seen in hibernating animals (Drew et al., 2013) would not be possible in seals as diving is typically associated with foraging.

Even though seals stop ventilation while diving, their tissues continue to metabolize, causing arterial O_2 content to decrease and arterial CO_2 content to increase (Scholander 1940). To extent the time of aerobic metabolism, diving mammals have enhanced tissue capacity to store oxygen both in blood and muscles (Scholander 1940; Burns et al., 2007; Blix et al., 2018). Hematocrit – percentage of blood volume that is occupied by erythrocytes – and blood hemoglobin concentration ([Hb]$_{blood}$) together with large blood volume are a crucial feature to optimize oxygen storage in blood (Burns et al., 2007). In deep diving phocid seals hematocrit can be as high as 60% and ([Hb]$_{blood}$) can reach levels > 25 grams/100 ml (Clausen and Ersland, 1969; Burns et al., 2007). However, maintaining high hematocrit is not possible without increased blood viscosity. Seals overcome this problem partially by storing their red blood cells in spleen while not diving, and these are then released into circulation when needed during diving (Cabanac et al., 1999). Overall, seals tend to have an increased blood volume (100-200 ml x kg^{-1}) compared to non-diving species (Lenfant et al.,1970). Consequently, this results in O_2 stores of blood that can be 3-4 times greater than average in terrestrial mammals (Blix, 2018).

Myoglobin (Mb) in muscles serves as an O_2 store as well due to its high affinity for oxygen (Wittenberg 1989). Swimming muscles of hooded seals have the highest (94 mg x g^{-1}) concentration of Mb recorded (Burns et al., 2007). More brain-spesific neuroglobin is a third protein, that possibly increases the neural oxygen stores (Burmester et al., 2000).

Diving animals respond to extended submersion by slowing their heart rate, a phenomenon known as bradycardia (Scholander 1940). This happens together with selective peripheral arterial vasoconstriction to ensure that the reduced cardiac output is preferentially directed to vital organs such as heart and the brain (Scholander 1940; Blix 1987; Blix 2018), and the seal brain seems to receive increased cerebral blood flow during episodes of hypoxia (Larson et al., 2014). However, vascularly mediated brain cooling under hypoxic conditions in seals appears to play a role as well, potentially decreasing cerebral oxygen demand by as much as 25% in these animals (Caputa et al., 1998; Odden et al. 1999; Blix et al., 2010).

However, despite the large body oxygen reserves and efficient oxygen utilization, deep-diving seals have still been shown to become severely oxygen-depleted while diving (Meir et al., 2009). Indeed, in the deep diving northern elephant seal (*Mirounga angustirostris*) experiences nearly complete blood O_2 depletion with every dive. This suggests that they, and

other deep-diving pinnipeds like hooded seals as well, are routinely exposed to extreme hypoxia (Meir et al., 2009).

1.4.2 Neural adaptations to hypoxia

As on the systemic level, complex coordination, and changes in various mechanisms together with partial shutdown is also needed on the cellular level during hypoxic conditions created by diving. This challenge is particularly critical for the nervous system due to its high dependency on oxygen, as previously discussed. To be able to tolerate hypoxia, mammalian nervous system must reduce metabolism, prevent cell damage, but still maintain functional integrity (Ramirez et al., 2007). In hypoxia tolerant animals, neural activity decreases in response to hypoxia in so called neural protective shutdown response, but returns during reoxygenation (Larson et al., 2014; Geiseler et al., 2016). Indeed, in hooded seal, during hypoxia genes involved in ion transport and other neuronal processes are downregulated, indicating the neuronal shutdown (Hoff et al., 2017).

Notably, seal neurons have been shown to be able to maintain stable membrane potential during severe hypoxia and therefore prevent excitotoxic cascade. In research from Folkow et al. (2008), where intracellular recordings were done in the pyramidal layer of isolated visual cortex slices, seal neurons were able to generate action potentials even after 60 minutes of severe hypoxia. Loss of membrane potential was also significantly larger in mice compared to seals, demonstrating that seal cortical neurons show remarkable intrinsic hypoxia tolerance which partly explains their ability to perform long dives, evidently without suffering from hypoxic injuries.

Since most of the brain's ATP consumption is used for maintaining ion gradients and stable membrane potential during synaptic transmission (Harris et al., 2012), it is very remarkable that it remains active in the hooded seal during hypoxia. Synaptic transmission was maintained in seals at 30% of the normoxic level amplitude for at least 3 hours of severe hypoxia (Geiseler et al., 2016).

Total understanding of mechanisms behind neural protective shutdown remains unclear, but there are multiple mechanisms suggested that might contribute. ATP sensitive potassium channels (K_{ATP} -channels) have been shown to attenuate neuronal excitability and excitatory neurotransmitter release (Fujimura et al., 1997; Ballanyi, 2004; Geiseler et al., 2015) and

neuromodulator adenosine seems to have neuroprotective functions (Rudolphi et al., 1992). However, in another hypoxia tolerant species, naked mole-rat (*Heterocephalus glaber*) synaptic transmission seems to be less affected by adenosine as in mouse (Larson and Park, 2009), which could be due to the altered presynaptic Ca^{2+} regulation in neurons of hypoxia tolerant mammals. Geiseler et al., (2016) showed attenuated paired pulse facilitation (PPF) in hooded seal hippocampus as well, possibly reflecting modified presynaptic Ca^{2+} regulation to reduce the detrimental effects of excessive Ca^{2+} influx. The PPF describes a phenomenon where a presynaptic neuron receives two stimuli rapidly and the postsynaptic response will commonly be larger in the second than in the first pulse (Schulz et al., 1994), suitable to investigate short-term synaptic plasticity (Zucker, 1989). In addition to hooded seal, it has been described in the naked mole-rat (Larson and Park, 2009). Reduced Ca^{2+} influx has been observed in other hypoxia-tolerant animals as well (Bickler and Gallego, 1993; Peterson et al., 2012) but exact mechanisms behind it remain to be clarified.

Altered neural metabolism might contribute to the shutdown response in seals together with other mechanisms. As earlier stated, there is evidence that mouse and rat neurons prefer lactate over glucose as fuel in normoxia. However, in seals the ANLS mechanism (see section **1.2**) is possibly reversed. Hypothesis is that due to the localization of mitochondria and neuroglobin in astrocytes oxidative metabolism seems to be located primarily in astrocytes instead of neurons in seals (Mitz et al., 2009, Schneuer et al., 2012). Benefit of this would be that it reduces the reliance of seal neurons on oxygen and prevents them from experiencing oxidative stress caused by mitochondrial activity (Turrens, 2003; Mitz et al., 2009). However, Gessner et al., (2022) have also shown increased expression of mitochondria related genes in hooded seal neurons, indicating their high capacity for aerobic metabolism. In addition to these other metabolic aspects, seal brain has three times higher glycogen stores compared to mouse brain, providing higher local energy stores (Czech-Damal et al., 2014).

1.5 Lactate and its many roles

Lactate, a product of anaerobic metabolism, was considered only as a metabolic product or a substrate in aerobic metabolism until recently. However, aside ANLS hypothesis, beneficial role of lactate in the brain has been suggested (Bergersen, 2015) and lactate seems to also have a supporting role during neuronal recovery after hypoxia (Schurr et al., 1988, Schurr, 2002). This holds up true only to a certain concentration of lactate. In seals, post-dive plasma

levels of lactate from 14 mM to 25 mM have been recorded (Scholander 1940; Kooyman et al., 1980; Kooyman et al., 1983), indicating a high tolerance to lactate. Indeed, the hooded seal brain has been shown to tolerate lactate levels up to 20 mM, whereas in mice neuronal activity rapidly vanishes (Czech-Damal et al., 2014), demonstrating that mice could not tolerate the levels of lactate that accumulate during diving in seals.

Lactate is also a link between metabolism and genes: lactylation of histones is a newly discovered epigenetic modification (Zhang et al., 2019). Histones are central components of chromatin, which is a structure of DNA and proteins. Chromatin organizes and regulates the genome, and histones in it can be altered by cellular enzymes by adding tags such as methyl, acetyl, and phosphate groups on them. These epigenetic alterations to the genome influence processes such as gene expression, DNA replication and repair (Peterson and Laniel, 2004). As mentioned, similar alteration by lactate has been found, leading linking metabolic events such as hypoxia where lactate is produced to gene expression (Izzo and Wellen, 2019; Zhang et al., 2019). Therefore, this metabolic regulation of gene expression could affect species that experience hypoxia on therefore lactate on a regular basis as well, such as hooded seal.

Aside from lactate's role in the genome and its well-known status as a metabolite, its role as a signaling molecule has started to emerge. The lactate-sensitive metabotropic receptor, HCAR1 (also referred to as GPR81, HCA_1), has been shown to be present both in human and rodent brain (Lauritzen et al., 2014; Briquet et al., 2022). This indicates that, in addition to being a metabolite and energy substrate, lactate also functions as a signaling substrate. HCAR1 was first cloned by Lee et al. (2001) and its specific agonist, lactate, was later identified in adipose tissue where it promotes lipid storage (Ge et al., 2008; Liu et al., 2009). HCAR1 was subsequently shown to be present in neurons (Lauritzen et al., 2014; de Casto Abrantes et al., 2019; Briquet et al., 2022), brain and pial blood vessels (Morland et al., 2017) and ventricular system as well (Hadzic et al., 2020). HCAR1 also seems to be concentrated at the postsynaptic membranes of excitatory-type synapses (Morland et al., 2015), but its precise localization in cells and regions in the brain remains unclear.

HCAR1 is a G-protein coupled receptor that has been shown to modulate neuronal network activity, possibly through cAMP modulation, and seems to have crosstalk with other GPCRs (Morland et al., 2015; de Castro Abrantes et al., 2019). Lactate has been shown to have neuromodulatory effect via HCAR1, decreasing synaptic activity in rodent brain (de Castro Abrantes et al., 2019; Briquet et al., 2022; Skwarzynska et al., 2023). In the human

brain, pharmacological activation of the receptor using non-metabolized agonist decreased the frequency of both spontaneous neuronal Ca^{2+} spiking and excitatory post-synaptic currents (Briquet et al., 2022). The same research suggested that hippocampal expression of HCAR1 is highest in the hilar area of the DG and in the pyramidal cells from CA3 region. However, there is indications that the antibody which was used is not HCAR1 specific since it is not knockout (KO) verified (personal communications, Geiseler, 2023).

Studies have also reported neurogenesis dependent on HCAR1 (Lambertus et al., 2021) and it has also been shown to be involved in enhanced brain angiogenesis linked with physical activity (Morland et al., 2017). Just recently, Skwarzynska et al. (2023) showed that metabolically generated lactate rapidly reduces neuronal excitability through HCAR1 both in vivo and in vitro. HCAR1 knockout (KO) mice were more likely to develop seizures than wild-type (WT) mice. The wide distribution and signaling effects of HCAR1 in the CNS suggest that the receptor may serve as a link between signaling, metabolism and blood (Morland et al., 2015).

The role of lactate as a signaling factor hasn't been investigated in hypoxia-tolerant animals such as hooded seal so far, but preliminary data suggests that lactate might be involved in neural protective shutdown in seals (Geiseler et al., unpublished).

1.6 Introduction to methlogy

1.6.1 Hippocampal fEPSP recordings

Electrophysiology is a neuroscience branch that explores electrical activity of living neurons and investigates processes related to their signaling. Neuronal activity can be investigated by recording spontaneous activity of the neurons, but recording evoked activity from hippocampal slices allows more specificity. Recording of evoked fEPSPs (field excitatory postsynaptic potentials) is a sensitive technique and it has been used to assess the effects of hypoxia challenge on brain tissue as well (Larson and Park, 2009; Geiseler et al., 2016). Extracellular field recordings measure responses from a population of neurons. When these neurons respond to stimulus and depolarize, synaptic activation is recorded. Since recording happens outside the cells, the synaptic signal is causing a negative deflection, indicating the flow of positive ions into postsynaptic neurons during synaptic transmission. The amplitude of the synaptic signal gives an indication of the depolarization of postsynaptic neurons (both

amount of activated synaptic connections and depolarization strength of individual postsynaptic membranes) and can therefore be used as an indication of synaptic transmission strength. Paired pulse ratio (see section 1.4.2) can be measured as well to investigate the short-term synaptic plasticity (Zucker, 1989; Larson and Park, 2009).

Geiseler et al. (2016) adapted the method of hippocampal evoked fEPSPs to the hooded seal, marking the first time it was applied to large mammals overall, despite the method is widely used in rodents. They also demonstrated that synaptic responses in reindeer are similar to those in mice, indicating that investigating hypoxia-related mechanisms via this method in seals is possible using mice as control despite the difference in body size.

"*As for many problems there is an animal on which it can be most conveniently studied*" (Krogh principle); the same can be applied on a tissue level. The hippocampus is one of the most thoroughly studied areas in the mammalian nervous system, both because of its role in learning and memory, and its distinctive structure. The unusual shape of the human hippocampus resembles that of a sea horse, which it is named after (in Greek hippos meaning "horse" and kampos meaning "sea monster") (Knierim, 2015). When studying energy consuming processes such as synaptic transmission, hippocampus is one of the prime examples of brain structures to use. It has a very clear, layered outline, making it easy to find and stimulate neural pathways and record synaptic corresponding responses.

The hippocampus forms a principally unidirectional network (**Figure 2**). To mention a few of them relevant to this project, neurons in the *Cornu Ammonis* 3 (CA3) region receive input from the Dentate Gyrus (DG) via mossy fibers. CA3 neurons send axons to the pyramidal cells of CA1 (*Cornu Ammonis* 1) via Schaffer collaterals (Daroff et al., 2014).
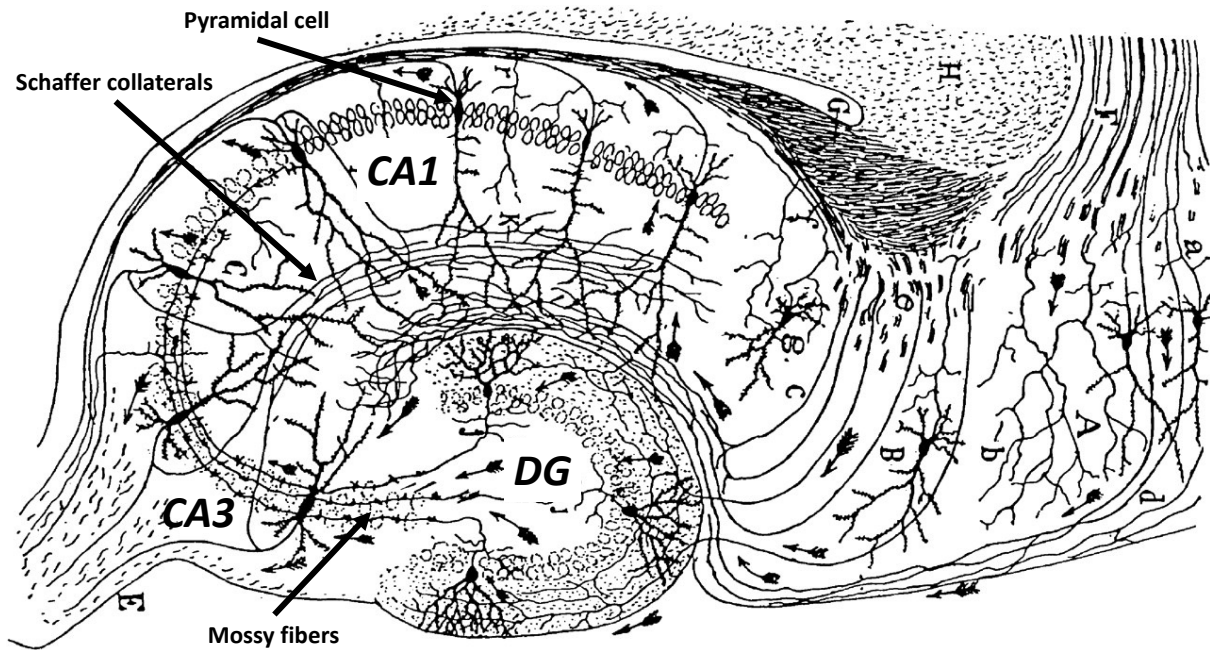
Figure 2 *Schematic view of neural circuitry of a rodent hippocampus, showing pyramidal cells, Schaffer collaterals, mossy fibers, regions CA1, CA3 and dentate gyrus (DG). Modified after Cajal (1911).*

Major excitatory (which make the postsynaptic neuron more likely to fire an action potential) and inhibitory (which make the postsynaptic neuron less likely to fire an action potential) neurotransmitters acting at directed synapses in hippocampus are glutamate and γ-aminobutyric acid (GABA). As previously described, glutamate actives receptors including AMPA and NMDA, whereas GABA activates $GABA_A$ and $GABA_B$ receptors (Daroff et al., 2014). Using the hippocampus as a model tissue therefore allows us also to investigate the roles of these neurotransmitters in particular. However, in this project we are investigating the excitatory responses only.

1.6.2 Real-time quantitative PCR (qPCR)

Real-time quantitative PCR (qPCR) is an efficient and common method for quantifying gene expression levels in a sample (Taylor et al., 2019). This quantification is achieved by measuring the copy number of a mRNA (messenger RNA) transcript from the target gene. The target gene is first reverse transcribed to complementary DNA (cDNA) from RNA using a reverse transcriptase enzyme. A sequency specific primer pair (of the gene of interest) is then used to amplify the target gene in a polymerase chain reaction (PCR) using a DNA polymerase enzyme, deoxyribonucleotide triphosphates (dNTPs) and fluorescent probes.

After each cycle of PCR, the fluorescence intensity is measured and used to determine the amount of amplified PCR-product generated, based on fluorescence intensity. The number of cycles before the fluorescence signal exceeds background levels and therefore the cycle threshold is referred to as cycle of quantification (Cq). During the analysis increase in fluorescence can be detected and amplification plot for each sample is created, showing curve of cycle number versus fluorescence signal (**Figure 3**) (Lager 2020). A greater amount of RNA transcript in the sample gives lower Cq -values, due to higher levels of PCR-product and therefore intensity of the fluorescence. In a relative quantification, samples are normalized to a stable expressed reference gene that is not regulated by the treatment of the samples (Bustin, 2000; Taylor et al., 2019).
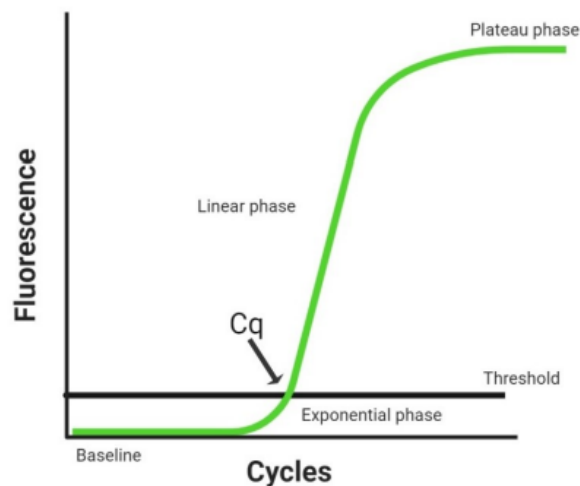
Figure 3 Amplification curve for one sample illustrating the different phases in the PCR reaction, with cycle number versus fluorescence signal. Indication of the Cq value where the fluorescence signal crosses an automatically generated threshold line indicated with an arrow. Illustration from Lager (2020).

Aims and hypotheses

The objective of this study is to investigate the potential role of lactate as a signaling molecule contributing to the neural protective shutdown in hypoxia-tolerant hooded seal. This aims to provide additional insights into the mechanisms underlying the neural shutdown response. By using mice as a control group, the study aims to uncover distinctions between hypoxia-tolerant and non-tolerant animals. As there is conflicting information regarding the localization of HCAR1 in the hippocampus, potential differences between the CA1 and CA3

regions (Briquet et al., 2022; personal communications, Geiseler 2023) will be examined to yield more comprehensive information.

Main hypothesis to be tested in this study:

Lactate contributes to the neural protective shutdown by suppressing neural activity via cerebral HCAR1 receptors in hooded seal.

Additional hypotheses to be tested:

a. Suppressing synaptic effect of lactate differs in hooded seal compared to non-hypoxia-adapted mouse.
b. There is no significant difference in synaptic response to lactate between the CA1 and CA3 regions of the hippocampus.

2 Methods

2.1 Overall research approach

Since expression of the HCAR1 receptor has not been investigated in the hooded seal brain before, the first part of my research was to examine the expression of this receptor using Real-time qPCR (Section **2.3**). After this, the second and major part of the research was to further investigate the role of the HCAR1 in hooded seal with method of electrophysiology, using field evoked post-synaptic potentials (Section **2.4**). The amplitude of the synaptic signals was recorded in the presence and in the absence of known agonists to the receptor, and these were then compared together. The same fEPSP experiments were performed to mice as well to use them as a control to compare a non-hypoxia tolerant species to a hypoxia tolerant one.

2.2 Animals and animal handling

2.2.1 Hooded seals

A total of six weaned hooded seal pups (**Table 1**) were live captured in their breeding colonies on the pack ice of the Greenland Sea at ~72°N and ~17°W during a scientific cruise on R/V Helmer Hanssen in March 2022, by approval from relevant Norwegian and Greenland

authorities. The animals were transported to Norway and kept in two 40 000-liter sea water pools in approved animal facilities at the Department of Arctic and Marine Biology, the Arctic University of Norway (approval number 089, the Norwegian Food Safety Authority (NFSA)). They were used for experiments in another project unrelated to the present one (permit number 29080). They were fed 2-3 kg herring (*Clupea harengus*) a day, supplemented with marine animal dietary vitamins and minerals (Sea Tabs ® MA, Pacific Research Labs Inc., CA, USA).

Hippocampal slices of all the animals were collected *postmortem*. The animals were euthanized in full isoflurane anesthesia by bleeding via the severed carotid arteries, as approved by NFSA (permit numbers 29013 and 29080), and as previously described (Geiseler et al., 2016).

      At the time of euthanasia, the seals were juveniles at 12-15 months of age. The pool was drained for capturing a seal, which was followed by an immediate sedation with intramuscular injection of zolazepam/tiletamine (Zoletil Forte Vet., Virbac S.A., France. 1.0-1.5 mg/kg of body mass). Seals were then anaesthetized via endotracheal ventilation with 2-3% isofluorane (Forene, Abbott, Germany) in air. After deep anesthesia was achieved, the animal was euthanized by cutting the carotid arteries. The dead seal was decapitated, and its skull was immediately placed in a bucket, filled with ice-cold oxygenated (95% O_2/5% CO_2, Linde Gas, Sweden) Ca^{2+}-free artificial cerebrospinal fluid (preparation aCSF) (**Table 11**) (Mathis et al., 2011). The skull was opened with a saw for accessing the brain unharmed. The opened skull with exposed brain was tranferred into another container with ice-cold oxygenated preparation aCSF within ~2 min of euthanasia. Within approximately 15 minutes after euthanasia, the hippocampus was dissected and cut into smaller pieces for further sample processing as described below (see section 2.4.1).

2.2.2 Mice

A total of 24 C57BL6 male mice aged 9-17 weeks (**Table 1**) were used. They were used for control purposes for this research as approved by NFSA (local *in vitro* project 01/23, approved by Vetenarian Amalie Andersen, AKM, UiT). The brain was extracted and transferred into ice-cold oxygenated (95% O_2/5% CO_2, Linde Gas, Sweden) preparation aCSF approximately 35 seconds after the death of the animal. Hippocampus was dissected

from both hemispheres of the brain for further processing, and continuously kept in ice-cold aCSF that was oxygenated (95% O_2/5% CO_2).

Table 1 *Sampled animals. Adult hooded seals that were used for another project but that provided isolated RNA samples for qPCR analysis (Section 2.3.1) on orange. Juvenile hooded seals on blue and mice on green.*

Species	ID	Age	Sex	Sampling date
Hooded seal	K1-15	adult	female	26.3.2015
Hooded seal	K2-15	adult	female	25.3.2015
Hooded seal	K3-15	adult	female	25.3.2015
Hooded seal	K8A-22	12 months	female	29.3.2023
Hooded seal	K9A-22	13 months	male	25.4.2023
Hooded seal	K3A-22	14 months	male	16.5.2023
Hooded seal	K10A-22	15 months	female	6.6.2023
Hooded seal	K7A-22	15 months	female	14.6.2023
Hooded seal	K2A-22	15 months	male	20.6.2023
Mouse	M1-23	10 weeks	male	3.3.2023
Mouse	M2-23	11 weeks	male	14.3.2023
Mouse	M3-23	11 weeks	male	16.3.2023
Mouse	M4-23	12 weeks	male	27.3.2023
Mouse	M5-23	12 weeks	male	31.3.2023
Mouse	M6-23	14 weeks	male	13.4.2023
Mouse	M7-23	15 weeks	male	18.4.2023
Mouse	M8-23	9 weeks	male	19.4.2023
Mouse	M9-23	9 weeks	male	20.4.2023
Mouse	M10-23	13 weeks	male	23.5.2023
Mouse	M11-23	13 weeks	male	25.5.2023
Mouse	M12-23	13 weeks	male	26.5.2023
Mouse	M13-23	13 weeks	male	30.5.2023
Mouse	M14-23	13 weeks	male	31.5.2023
Mouse	M15-23	14 weeks	male	1.6.2023
Mouse	M16-23	14 weeks	male	2.6.2023
Mouse	M17-23	14 weeks	male	8.6.2023
Mouse	M18-23	14 weeks	male	9.6.2023
Mouse	M19-23	15 weeks	male	13.6.2023
Mouse	M20-23	17 weeks	male	26.6.2023
Mouse	M21-23	17 weeks	male	26.6.2023
Mouse	M22-23	17 weeks	male	27.6.2023
Mouse	M23-23	17 weeks	male	27.6.2023
Mouse	M24-23	17 weeks	male	28.6.2023
Mouse	M25-23	17 weeks	male	28.6.2023

2.3   Real-time quantitative PCR (qPCR)

Real-time qPCR was done to show the presence of the mRNA of HCAR1 in the hooded seal CNS (hippocampus, cerebellum, and visual cortex), which would confirm that the target receptor exists in the hippocampus of this species as well. Since the qPCR experiments were done in advance before starting with the electrophysiology experiments, the isolated RNA

samples for cDNA synthesis were provided from previous sampling done in 2015 (Geiseler et al., 2016) as described in section **2.3.1**. cDNA synthesis was done to these samples to transform the RNA into cDNA for the qPCR analysis (Section **2.3.2**). Before performing the qPCR analysis, primers were optimized (Section **2.3.3**). After this, the qPCR analysis itself was performed (Section **2.3.4).**

Other hypoxia related genes were sampled and analyzed together with HCAR1, but this was for purposes outside the scope of this project, which is why the results of them are not presented or discussed.

2.3.1   Animals, samples, and sampling procedures

Since qPCR experiments were done in advance before starting with electrophysiology experiments, RNA samples (**Table 2**) for cDNA synthesis were provided from sampling done for a previous project (Geiseler et al., 2016), see adult animals included in **Table 1**. Hippocampal slices were collected from animals *postmortem* and euthanasia was conducted in accordance with approvals obtained from the National Animal Research Authority of Norway (NARA; approval numbers 7247, 6216, 5399). Further explanation of the procedure provided in Geiseler et al (2016). Seal hippocampi samples were first incubated for a 20-minute adaptation period, followed by 60 minutes of hypoxia (95% N_2/5% CO_2) or normoxia (95% O_2/5% CO_2; control). After incubation the samples were stored in RNAlater before RNA extraction using RNeasy Plus Universal Mini Kit (QIAGEN, Hilden, Germany), genomic DNA was removed by treating the RNA with Ambion TURBO Dna-free™ Kit (Life Technologies, CA, USA) and concentration of RNA was measured using NanoDrop ND2000c (Thermo Scientific, MA, USA) (Geiseler et al., 2016) (**Table 2**). Isolated RNA was stored in -80°C.

2.3.2   cDNA synthesis

cDNA synthesis was done to the isolated RNA samples (**Table 2**) to transform the RNA into cDNA. Synthesis was done using High Capacity cDNA Reverse Transcription Kit for 200 and 1000 reaction kits by Applied Biosystems.

Total volume for each cDNA synthesis tube (Eppendorf) was 10 µl. Volume of RNA sample that should be added to the cDNA sample tube was calculated based on the measured RNA concentration to achieve optimal concentration used in the Kit (1000ng/10µl per each sample). Rest of the volume (10 µl) was distilled water, and it was added to the tubes first. Calculated RNA volume was added after this.

Table 2 RNA samples with their sample codes and numbers for cDNA synthesis. Measured concentrations and possible dilutions included. Portions of RNA and H_2O in the sample tubes are shown. In the sample codes: HC = hippocampus, Ce = cerebellum, VC = visual cortex, H = hypoxia, N = normoxia.

Sample code	Measured RNA concentration (ng/µl)	µl of RNA sample	µl of distilled H_2O
K1-15-H-HC	481.1	2.1	7.9
K2-15-H-HC	622.3	1.6	8.4
K3-15-H-HC	617.8	1.6	8.4
K1-15-N-HC	613	1.6	8.4
K2-15-N-HC	523.6	1.9	8.1
K3-15-N-HC	708	1.4	8.6
K1-15-H-Ce	393.2	2.5	7.5
K2-15-H-Ce	826.5	1.2	8.8
K3-15-H-Ce	520.7	1.9	8.1
K1-15-N-Ce	592.1	1.7	8.3
K2-15-N-Ce	356.2	2.8	7.2
K3-15-N-Ce	692.4	1.4	8.6
K1-15-H-VC	616.7	1.6	8.4
K2-15-H-VC	407.9	2.5	7.5
K3-15-H-VC	302.1	3.3	6.7
K1-15-N-VC	256.8	3.9	6.1
K2-15-N-VC	506.2	2.0	8.0
K3-15-N-VC	826	1.2	8.8

cDNA synthesis mixes were made for the samples. Mixes contain chemicals that are needed for the cDNA synthesis. Unlike RT plus mix (**Table 3**), RT minus mix (**Table 4**) does not include the reverse transcription enzyme and replicate samples mixed with it work as a control to indicate the efficiency and reliability of the cDNA synthesis.

10 µl of plus mix was added to each RNA sample tube and mixed by pipetting 3-4 times. 10 µl of minus mix was added to the four additional randomly chosen minus sample tubes and mixed by pipetting 3-4 times. The rest of the procedure was done same to all the samples, both in minus and plus mixes. All the tubes were incubated for 10 minutes at 25°C, and then for 2 hours at 37°C. After this they were incubated for 5 minutes at 90°C and then cooled down. Tubes were centrifuged and 60 µl of water was added to each tube. Tubes were stored in -20°C for later analysis.

Table 3 Plus mix for cDNA synthesis.

Reverse transcription (RT) plus mix	Per one sample (µl)
10 x RT Buffer	2
25 dNTP	0,8
10 x Random primer	2
RT enzyme	1
H_2O	4,2

Table 4 Minus mix for cDNA synthesis.

Reverse transcription (RT) minus mix	Per one sample (µl)
10 x RT Buffer	2
25 dNTP	0,8
10 x Random Buffer	2
H_2O	5,2

2.3.3 Primer optimization

Primers are designed to copy specific targeted segments of mRNA (cDNA) and they define the product (amplicon) that is generated in the PCR reaction (Taylor et al., 2019) which in case of this project is mRNA for HCAR1 in hooded seal and the reference gene primers. Primer design was performed by the Cardiovascular Research Group (IMB, UiT) prior to the start of this project. Primer pairs for qPCR were designed from the obtained nucleotide sequences using NCBIs Primer-BLAST, which was also used to predict primer products based on the genome of a related pinniped species, Weddell seal (*Leptonychotes weddelii*)

(GCA_000349705.1). The primer oligos were purchased from Sigma-Aldrich (UK) and their specific sequences can be found on **Table 5**. The reference genes used were those that were not regulated by the treatment of the samples (for treatment, see section **2.3.1**). The selected reference genes, identified as the most stable in the samples (see **Virhe. Viitteen lähdettä ei löytynyt.**, **Virhe. Viitteen lähdettä ei löytynyt.** and **Table S 1** in Appendix A) and that were used included HPRT1, TBP and GAPDH.

Table 5 *List of primers used in the qPCR analysis. Accession numbers from genomes of a related pinniped species, Weddell seal. FP = forward primer, RP = reverse primer.*

Gene symbol	Gene name	Accession number	Sequence (5'-3')
HCAR1	hydroxycarboxylic acid receptor 1	NW_006384524.1	FP: GACGCTCCAAGACCCAGAGG RP: GGCTCTGGAAGCCATTTGCC
HPRT1	Hypoxanthine phosphoribosyltransferase 1	XM_045882778.1	FP: ACTGGCAAAACCATGCAAACC RP: CAAACTTGCGACCTTGACCA
TBP	TATA-box binding protein	XM_006744636.2	FP: AACAGCCTGCCGCCTTATG RP: TGCCGTAAGGCATCATTGGA
GAPDH	Glyceraldehyde-3-phosphate dehydrogenase	XM_045873995.1	FP: ACACGGAAGGCCATGCCAG RP: CCTCTGGGAAGCTGTGGC

Primer optimization was done to test different concentrations and to find the most optimal concentration for each primer to be used in the qPCR analysis. Stock solution of 200 μM was made of each primer and a working solution of 10 μM was made from this with 20 μl of prime stock solution and 380 μl of double distilled water. These both were stored at -20°C when not used.

Four dilutions of the working solutions – forward (Fp) and reverse (Rp) primer for each gene – were prepared (**Table 6**) so that the end concentration of primers in the PCR wells would be 100-800 nM.

Table 6 Working solutions for primer optimization.

Concentration	Forward primer	Reverse primer	Double distilled water
100 nM	5 μl	5 μl	90 μl
200 nM	8 μl	8 μl	64 μl
400 nM	14 μl	14 μl	42 μl
800 nM	22 μl	22 μl	11 μl

Primer optimization plus master mix was prepared (**Table 7**). Minus master mix was prepared to control the accurancy of the analysis (**Table 8**) by having parallel sample of primer with minus mix. 8 μl of master mix was added to each well in the PCR plate and 2 μl of primer solution after that. Plate was analyzed using Roche LightCycle96 (Hoffmann-La Roche Ltd, Switzerland).

Table 7 Primer optimization plus mix

Primer optimization plus mix	Per sample
SYBR green (Roche)	5
cDNA	2
Distilled H$_2$O	1

Table 8 Primer optimization minus mix

Primer optimization plus mix	Per sample
SYBR green (Roche)	5
Distilled H$_2$O	3

2.3.4 Real-time PCR: Gene quantification

Real-time PCR was done using FastStart SYBR Green Master Kit from Roche (Hoffmann-La Roche Ltd, Switzerland). To measure the efficiency of the PCR reaction, cDNA pool dilution series was done from all samples in the experiment. cDNA pool was done by adding 5 μl from each plus mix sample. Dilution series 1:5 was done by adding 20 μl of water to each tube and then 5 μl of sample from the previous dilution (**Table 9**).

Table 9 *Dilution series of cDNA pool for the qPCR analysis.*

Dilution	cDNA concentration
cDNA pool	100 %
Dilution 1	20 %
Dilution 2	4 %
Dilution 3	0,8 %

Master mixes (**Table 10**) were prepared to quantify the target and reference genes. Each cDNA sample (**Table 2**) had a replication on the PCR plate. 8 µl of master mix was added to each well of the PCR plate, followed by adding 2 µl of sample to make the total volume 10 µl. 2 µl of cDNA pool and 2 µl of each of its dilution (**Table 9**) was added to their own wells. All plates were analyzed in Roche LightCycle96 (Hoffmann-La Roche Ltd, Switzerland), approximately for 1 hour and 10 minutes.

Table 10 *Master mixes for qPCR per sample depending on the optimized primer concentration. Primer concentrations for the target were following: GAPDH = 400 nM, HPRT-1 = 400 nM, TBP = 800 nM and HCAR1 = 400 nM.*

	Primer concentration (400 nM) per sample	Primer concentration (800 nM) per sample
SYBR green (Roche)	5 µl	5 µl
Forward primer	0,4 µl	0,8 µl
Reverse primer	0,4 µl	0,8 µl
H_2O	2,2 µl	1,4 µl

2.4 Electrophysiology

2.4.1 Set-up and sample preparation

2.4.1.1 Buffers/tissue media

Artificial cerebrospinal fluid (aCSF) (Mathis et al., 2011) was prepared the day before the experiments. Ingredients were weighted and mixed in container with distilled water. aCSF

was oxygenated (95% O_2/5% CO_2, Linde Gas, Sweden) and pH was measured to be 7,4 with pH-meter (pH 1000 H, VWR International LLC). Preparation aCSF (prep aCSF) used for dissection was made to have 30 mM concentration of glucose, standard aCSF (std aCSF) used for experiments and holding chambers had 10 mM glucose and 20 mM sucrose concentration and finally the lactate aCSF used for lactate experiments had 20 mM lactate and 10 mM glucose concentration (see section 1.5, Scholander, 1940; Kooyman et al., 1980, Kooyman et al., 1983; Mathis et al., 2011; Offermanns, 2017). Ice-cold Ca^{2+} free prep aCSF was used to slow metabolism and minimize the Ca^{2+} dependent excitotoxicity during dissection of the brain (Mathis et al., 2011). Composition of all the types of aCSF are shown in **Table 11**.

Table 11 Composition of aCSF. All the types of aCSF included salts of the stock section. Standard aCSF also included 10 mM glucose with 20 mM sucrose, preparation aCSF 30 mM glucose and lactate aCSF 20 mM lactate with 10 mM sucrose.

		Molecular weight	Concentration (mM)	g / 1 liter	Producer
Stock	**NaCl**	58.442	128	7.48	Sigma-Aldrich
	KCl	74.55	3	0.22	Merck
	NaH₂PO₄ x H₂O	137.99	0.5	0.068	Sigma-Aldrich
	NaHCO₃	84.01	24	2.02	Sigma-Aldrich
	CaCl₂	111.01	3.5	0.389	Sigma-Aldrich
	MgCl₂	95.21	1.0	0.10	Merck
Standard aCSF	**D(+) glucose**	180.16	10	1.8	Sigma-Aldrich
	Sucrose	342.3	20	6.85	Sigma-Aldrich
Preparation aCSF	**D(+) glucose**	180.16	30	5.4	Sigma-Aldrich
Lactate aCSF	**Na-Lactate**	112.06	20	2.24	Sigma-Aldrich
	Sucrose	342.3	10	3.42	Sigma-Aldrich

2.4.1.2 Tissue slicing, bath, perfusion and oxygenation

The freshly dissected hippocampal tissue was glued (Loctite Superglue, Henkel, Germany) onto the stage of a vibratome (Leica VT1000 S, Leica Microsystems Nussloch Gmbh, Germany). The transverse slices were supported and made steady with pieces of 4% agarose (VWR International Ltd., Lutterworth, UK). The slicing was performed in ice-cold oxygen-bubbled (95% O_2/5% CO_2, Linde Gas, Sweden) prep aCSF. In seals, produced slices were cut 400 μm thick (Geiseler et al., 2016) and had 4-5 mm diameter. Slices from mice had diameter of ~0.5 mm with the same thickness as in seals. After the cutting, the slices were transferred

to holding chambers at room temperature (~20°C) containing oxygenated std aCSF. When all the slices were transferred, aCSF in the chambers was slowly warmed from room temperature of ~20°C to 37°C.

For the experiments the slices were moved to a 20 ml volume acrylic recording chamber that was filled and circularly perfused with std aCSF at a rate of 30 ml per minute. The chamber was connected to a jacketed and temperature-controlled glass container, and altogether the volume of the system was 200 ml. The glass container was warmed up from a water bath to maintain a temperature of 37°C of aCSF circulating in the system. Nylon net was placed and submerged in the recording chamber, and the hippocampal slices were placed on top of the net to allow access of oxygenated std aCSF to both sides of the slice. Slices were given at least 30-minute time to get equilibrate to these conditions, before any recordings were started.

2.4.1.3 Electrophysiological recordings

Recording micropipettes were pulled from glass capillaries (OD = 1.50 mm, ID 0.86 mm, length 10 cm, Warner Instruments, MA, USA) using micropipette puller (P97 Flaming/Brown, Sutter Instrument Co., USA) and filled with [6 M] NaCl. Signal from the slices was transferred via the electrolyte (6 M NaCl) to the recording electrode and further to the recording units. Bipolar stimulating electrodes were made from isolated NiCr wire (50 μm bare diameter, A-M Systems, WA, USA). Stimulation of the slices was provoked using a computer-controlled 8-channel stimulator (Model 3800, A-M Systems, WA, USA) that was coupled with a stimulus isolation unit (Model 3820, A-M Systems, WA, USA). Strength of the stimulation for each experiment was modified depending on each slice, varying in mice from 30 to 150 μA, and in seals between 80-180 μA. The recorded signal was amplified via headstage and amplifier that both amplify the signal ten times (Model 3000, A-M systems, WA, USA). The signal was filtered with high pass of 0.1 Hz and low pass of 3 kHz, followed in an Analogue-/Digital signal converter (PowerLab 4/25, ADInstruments Ltd, Dunedin, New Zealand). Recordings and and the initial analyses of all signals were done using LabChart 7.0 (ADInstruments Ltd, Dunedin, New Zealand).

Experiments included field recordings done on two different *Cornu Ammonis* (CA) regions of the hippocampus, CA1 and CA3 (see section 1.6.1). In CA1 experiments, stimulation

electrode was positioned in the *stratum radiatum* of CA1c subfield for activation of the Schaffer-commissural fibers. The recording electrode was placed in the *stratum radiatum* of CA1b to record the field excitatory postsynaptic potentials (fEPSPs) between Schaffer commissural fibers and pyramidal neurons (**Figure 4A**). In the CA3 experiments the stimulating electrode was placed in dentate gyrus to stimulate mossy fibers, and micropipette was placed to measure potentials between mossy fibers and pyramidal cells in the CA3 region (**Figure 4B**). Due to technical challenges of dissecting and cutting the hippocampal slices without damaging the CA3 region and finding the right position of the electrodes in the slices from seal, experiments in the CA3 -region were only done in mice and not in the hooded seals.
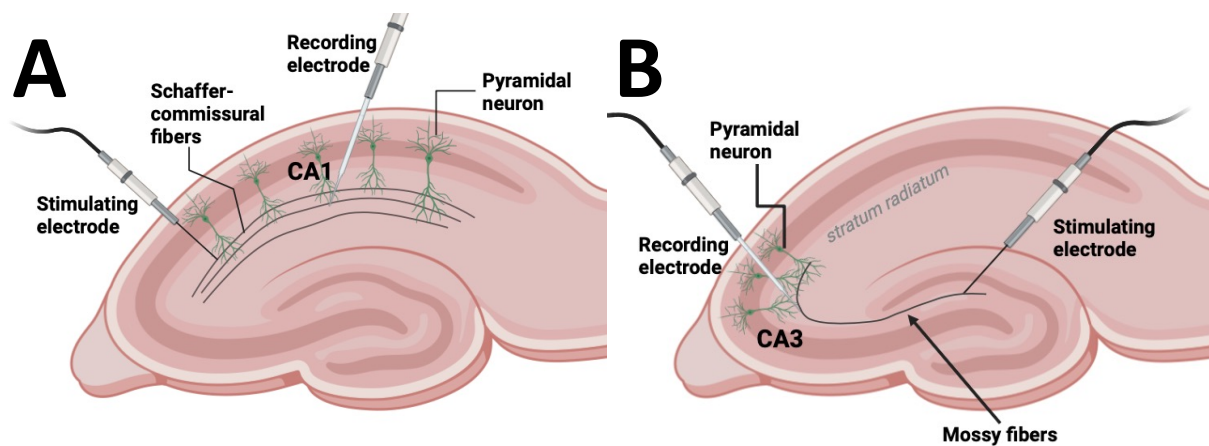
Figure 4 *Simplified schematic of synaptic organization and placement of electrodes in CA1 and CA3 regions. A) Placement of the electrodes in the CA1 region experiments. Stimulating electrode was placed in the stratum radiatum of CA1c subfield to activate Schaffer-commissural fibers, and glass-recording electrode was positioned in the CA1b to record the potentials. B) Placement of the electrodes in the CA3 region experiments. Stimulating electrode was placed to activate mossy fibers and recording electrode in the CA3 to measure potentials between pyramidal cells and mossy fibers. Figures created with BioRender,*

fEPSPs were evoked in all the slices at 10 second intervals through the experiments with constant recordings. To include investigation of paired pulse variations recordings were done using inter-pulse interval (IPI) (see section **1.6.1**) of 10 ms and 75 ms. However, analysis of this is not included in this thesis due to time limitation (see section **2.4.2.2**). Evoked responses were digitalized and analyzed using LabChart 7.0.

2.4.2 Protocols

2.4.2.1 Main experiments

Experiments were conducted in normoxic conditions (oxygenation of aCSF with 5% O_2/95% CO_2, Linde Gas, Sweden), by studying synaptic responses in mouse and seal hippocampal slices while adding agonists of the HCAR1 lactate receptor. Baseline recordings were taken for at least 10 minutes before any potential agonists were added, and before this the slices were given sufficient equilibration time (5-15 minutes) after placing the electrodes to make sure that the signal was stable. Baseline recording consisted of recordings both with IPI of 10 ms and 75 ms. Activation of the receptor was introduced in three different ways: using agonist 3Cl-HBA (3-Chloro-5hydroxybenzoic acid, Tokyo Chemical Industry Co., Ltd., Tokyo, Japan) using agonist 3,5-DHBA (3,5-Dihydroxybenzoic acid, Sigma-Aldrich, Darmstadt, Germany) or by changing to 20 mM lactate aCSF (de Castro Abrantes et al., 2019). 3Cl-HBA was mixed with vehicle dimethyl sulfoxide (DMSO, Sigma Aldrich) before adding it to the system. All the drugs were mixed on the same day of the experiments. In both artificial agonist experiments, concentration of the drug was increased four times, starting with known working concentration for mice (de Castro Abrantes et al. 2019) (**Table 12**). Since the 3,5-DHBA experiments on mice were done in the very beginning, the concentration was increased from 1 mM to 8 mM to find working concentration for our system. Recordings were done in subsequent intervals. Each interval consisted of recordings for 10 minutes with IPI 10ms plus 2 minutes with IPI of 75ms. Stimulations were done in 10 second intervals to avoid network artifacts (Larson and Park, 2009). Concentration of agonist was doubled for each interval, ranging from 1 mM to 4/8 mM in 3,5-DHBA and from 40 µM to 320 µM in 3Cl-HBA. After the last interval, the system was rinsed with fresh std aCSF. After at least 400 ml of 37°C aCSF had gone through the system (~13 minutes), the rinsed effect recording was made. The lactate experiments had the same basic protocol, except the aCSF was changed only once to the 20 mM lactate aCSF (physiological concentrations, e.g. Kooyman et al., 1983; Offermanns, 2017).

Table 12 Concentrations of agonists and Na-lactate in aCSF in the experiments. * = Concentration of the 3,5-DHBA agonist was increased up to 8 mM in aCSF only in mice experiments. In the seal experiments highest concentration that was used was 4 mM.

	Concentration
Na-Lactate	20 mM
3,5-DHBA	1 mM, 2 mM, 3 mM, 4 mM, 8mM*
3Cl-HBA	40 µM, 80 µM, 160 µM, 320 µM

To verify that the response was indeed an excitatory glutamatergic response and not an artifact, some of the experiments were always ended by adding AMPA-type glutamate receptor antagonist CNQX (disodium salt hydrate, Sigma Aldrich) to 25 μM in the aCSF (Blake et al., 1988; Geiseler et al., 2016). CNQX blocks the post-synaptic AMPA-channels and therefore also EPSP (Blake et al., 1988), verifying the signal to be synaptic. Control experiments were done by adding 1 ml of the drug vehicle, DMSO in the system (70 mM) after the baseline recording and doing a recording for at least 10 minutes following this. All the experiments were done on slices from different animals, except in the seal DMSO control experiments all the slices were from the same animal due to animal availability.

2.4.2.2   Additional experiments

Separate experiments were done to examine the potential hypoxia-protective roles of both adenosine (Heit et al., 2021) and K_{ATP}-channels (Geiseler et al., 2015) (see section 1.4.2). In this context, A1 adenosine antagonist 8-cyclopentyl-1,3-dipropylxanthine (CPX, Sigma-Aldrich) was used to see if any adenosine-induced the attenuation of synaptic transmission could be reversed. Adenosine experiments were done both in hooded seals and mice. Investigation of K_{ATP}-channels in hooded seals included three different experiments: effect of K_{ATP}-channel blocker tolbutamide (Supelco, Sigma-Aldrich, Geiseler et al., 2015) in hypoxia, effect of K_{ATP}-channel agonist diazoxide (Sigma-Aldrich, Geiseler et al., 2015) in normoxia and effect of tolbutamide and diazoxide together in normoxia. Episodes of hypoxia were conducted by replacing the O_2 supply to the perfusion aCSF with nitrogen (95% N_2/5% CO_2, Linde Gas, Norway).

In addition, incubation experiments were done to excess tissue from electrophysiology experiments to investigate the cellular mechanisms of the seal hippocampus during normoxia, hypoxia and during reoxygenation. Cutting was done in oxygenated (95% O_2/5% CO_2, Linde Gas, Sweden) prep aCSF and the experiments in std aCSF. The transverse hippocampal slices (1-2 mm) were cut with scalpel, and another cut was done to separate CA1 and CA3 regions into two different tissue samples. This was to investigate possible differences in the expression of the HCAR1 receptor between CA1 and CA3 regions of hippocampus. These incubation experiments were done in the same way as described in section 2.3.1, but in addition to 60 minutes of hypoxia (95% N_2/5% CO_2, Linde Gas, Norway), 20 minutes of reoxygenation (95% O_2/5% CO_2, Linde Gas, Sweden) time was included (and as a control to

that, 80 minutes of normoxia (95% O_2/5% CO_2)). After the incubation, slices were moved to RNAlater tubes and stored in -80°C.

Analysis of both the separate fEPSP experiments and incubation experiments are beyond the scope of my thesis due to time limitations, but they were done to optimize both the use of the animals and the rare possibility to do research on them. In addition, they are highly relevant in terms of investigating the neural protective shutdown mechanisms in hooded seal.

List of animals and experiments performed on them can be seen on the **Table 13**.

Table 13 Experiments done on the animals. Green = analyzed experiment, red = failed experiment, blue = unanalyzed experiment.

Species	ID	qPCR	Incubation	3,5-DHBA, CA1	3,5-DHBA CA3	3Cl-HBA	Lactate 20mM	Adenosine	Tolbutamide	Diazoxide	Tolbutamide + diazoxide	DMSO control
Hooded seal	K1-15	green										
Hooded seal	K2-15	green										
Hooded seal	K3-15	green										
Hooded seal	K8A-22		green	green		green	green	blue				
Hooded seal	K9A-22		green	red		red	green	blue	blue	blue	blue	
Hooded seal	K3A-22		green	green		green	green	blue	blue	blue	blue	
Hooded seal	K10A-22		green	green		green	green		blue	blue	blue	
Hooded seal	K7A-22		green				green	blue	blue	blue	blue	
Hooded seal	K2A-22		green	green		green	green		blue	blue	blue	green
Mouse	M1-23			green		red						
Mouse	M2-23			green								
Mouse	M3-23				green		red					
Mouse	M4-23			green								
Mouse	M5-23				red			blue				
Mouse	M6-23				red		green					
Mouse	M7-23				red		red					
Mouse	M8-23						red					
Mouse	M9-23			red	red							
Mouse	M10-23			red	green							
Mouse	M11-23			red		green	green					
Mouse	M12-23					green						
Mouse	M13-23					red	green					
Mouse	M14-23					red						
Mouse	M15-23					green						
Mouse	M16-23				green							
Mouse	M17-23				red	green	green					
Mouse	M18-23							blue				
Mouse	M19-23											green
Mouse	M20-23											green
Mouse	M21-23							blue				green
Mouse	M22-23							blue				red
Mouse	M23-23							blue				green
Mouse	M24-23							blue				

2.5 Data analyses

2.5.1 qPCR

The Cq values obtained from the Light Cycler96 Software were used to calculate expression the gene levels in the samples. Relative quantification was used, meaning that sample (HCAR1) was normalized to global mean of stable expressed reference genes (GAPDH, HPRT1, TBP), resulting in a unitless ratio of gene levels. Relative quantification was done using qPCR Data Analyzer Excel-file programmed by Knut Steinnes (Lab engineer, UiT). The efficiency of the PCR reaction was counted from the serial dilution of the cDNA pool from samples in the experiments (see section **2.3.4**) using the software (Light Cycler96) that automatically generates the efficiency value.

2.5.2 Electrophysiology

Data was extracted using LabChart 7.0 and Microsoft Excel (version 16.78, 2023). Amplitude of the signal was measured 0.2 milliseconds before the stimulus to get the baseline at that point of the recording (**Figure 5**, part 1). This was to get the baseline value as close to the EPSP as possible, but without capturing the stimulus. Amplitude of the synaptic signal was measured to be the lowest point between 2 milliseconds to 7 milliseconds after the stimulus (**Figure 5**, part 2). To get the actual amplitude of the fEPSP, the measured baseline value was subtracted from the amplitude of the synaptic signal. This was done to all the fEPSPs. As mentioned before, paired pulse protocol was in use but only the first fEPSP in each paired stimulation was measured in the context of the HCAR1 experiments. Analysis of the paired pulse stimulation data is left out from this thesis due to time limitation (see section **2.4.2.2**).
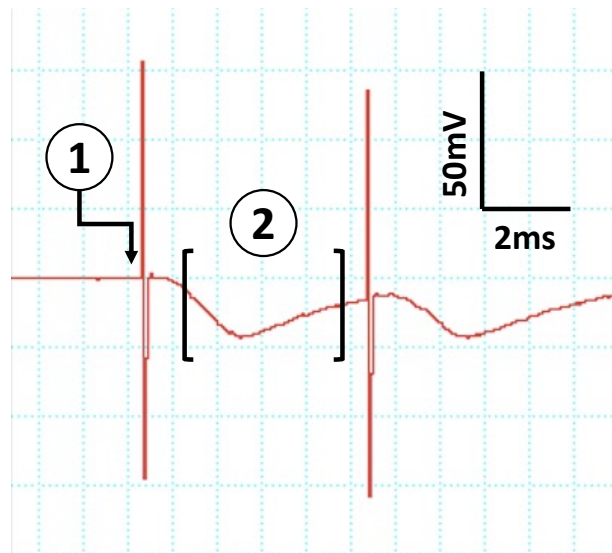
Figure 5 *Representation of example fEPSP signal from LabChart with indications of the time periods at which the amplitude of the signal was measured. Y axis presents the signal amplitude (mV) against time (ms). 1) Baseline amplitude that was measured 0.2 milliseconds before the stimulus to get the baseline value. 2) Amplitude of the synaptic signal was measured to be the lowest point of the recording between 2-7 milliseconds after the stimulus – this period is indicated by the brackets.*

Extracted raw data was further analyzed by counting the average of fEPSP amplitude for a 3-minute period for each treatment in each slice. **Figure 6** illustrates how the analysis was done in lactate experiments. In the non-metabolic agonist (3,5-DHBA and 3Cl-HBA) experiments analysis was done the same way, except each concentration had its own measurement, and the middle point of the 3-minute period was located 4 minutes and 20 seconds after an increase in the concentration. Since the slices were stimulated every 10 seconds, each mean value representing treatment was calculated from 18 data points.
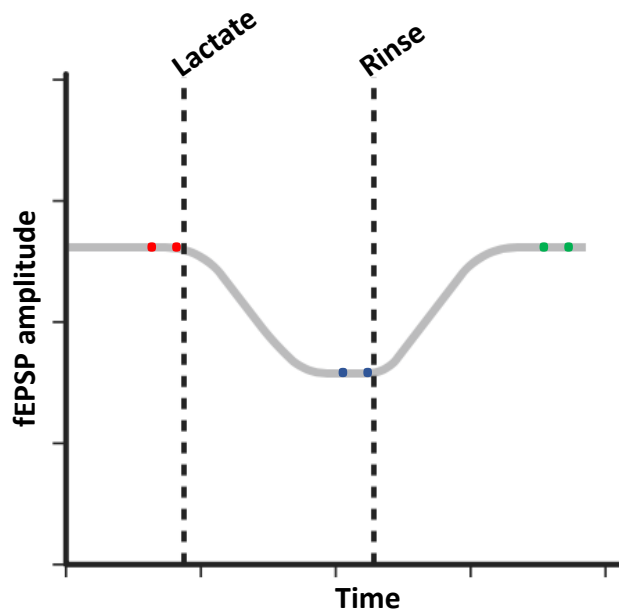
Figure 6 *Illustrative figure demonstrating the data extraction from raw data of lactate experiment. Y axis represents fEPSP amplitude and X axis time. Change of treatment is indicated with the lines, and each measured 3-minute period is within the dots (red = baseline, blue = lactate, green = after rinsing).*

Mean values for each treatment were normalized to the baseline average voltage recorded in each slice, which was set to be 100%.

2.5.3 Statistics

Data was first tested for normal distribution. Repeated measures one-way ANOVA with multiple comparisons (Tukey) was used to compare the effects of agonists and lactate to the baseline recordings and recordings after rinsing. Differences between animal groups were tested using unpaired t-tests. In all tests P-value <0.05 was considered significant. All statistical analyses and formulating of result graphs were performed using GraphPad Prism (version 10.0.3 for Windows (2023), GraphPad Software, MA, USA).

3 Results

3.1 HCAR1 mRNA is expressed in the brain of hooded seal

Relative quantification of the gene levels using qPCR showed expression of HCAR1 mRNA in the hooded seal CNS (hippocampus, cerebellum, visual cortex) both in hypoxia and

normoxia when normalized to the reference genes GAPDH, HPRT-1 and TBP (**Figure 7**). In hippocampus, mean of mRNA levels of HCAR1 was higher in the hypoxia incubated samples (0.00347±0.00139) compared to the normoxic samples (0.00265±0.00049). In cerebellum mean value was the same (normoxia 0.00144±0.00022, hypoxia 0.00144±0.00024). In visual cortex, mean value for mRNA levels in normoxia (0.00929±0.00449) were higher compared to hypoxia (0.00273±0.00053). There was no statistically significant difference between any the samples (p=0.1114, n=3 seals).
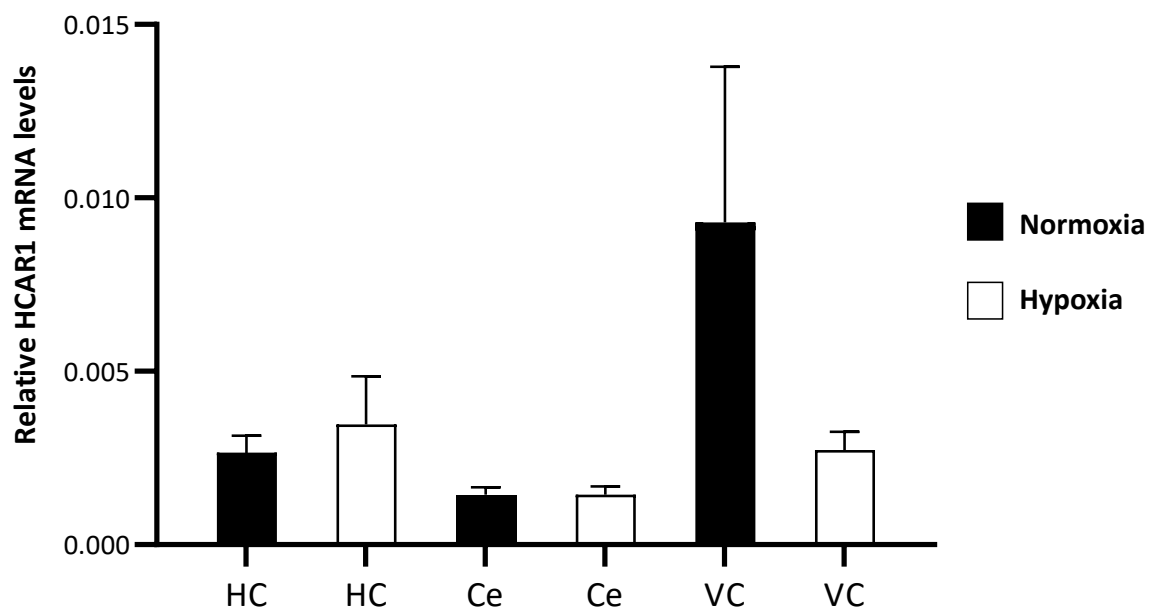
Figure 7 *The mean relative mRNA levels of HCAR1 in hooded seal CNS during normoxia and hypoxia. Y-axis represents mRNA levels (unitless ratio with relative quantification) of HCAR1 normalized to the global mean of the reference genes (GAPDH, HPRT-1, TBP), and each bar shows a sample of brain region in different treatments (HC=hippocampus, Ce=cerebellum, VC=visual cortex). Error bars show standard error of mean.*

3.2 Extracellular evoked fEPSP recordings

Experiments were conducted to test the hypothesis that lactate contributes to the neural protective shutdown by diminishing neural synaptic activity via cerebral HCAR1 receptor. The field excitatory post-synaptic potentials (fEPSPs) of hooded seal and mouse hippocampal slices had size and shape that has been reported in studies from other laboratories and previous experiments (e.g., Sebastião et al. 2001; Larson and Park, 2009; Geiseler et al., 2016). The baseline values ranged from 16-54 mV in hooded seals and 7-65 mV in mice. Due to the impossibility with evoked field EPSP recordings to always stimulate and record exactly

the same number of synaptic connections, the baseline values before start of any treatment were normalized and set to 100% (Henze et al., 2000; Sebastião et al. 2001).

During control experiments there was no effect on the amplitude of fEPSP signal after adding DMSO (70mM) in hooded seal (**Figure 8**) or mouse (**Figure 9**).
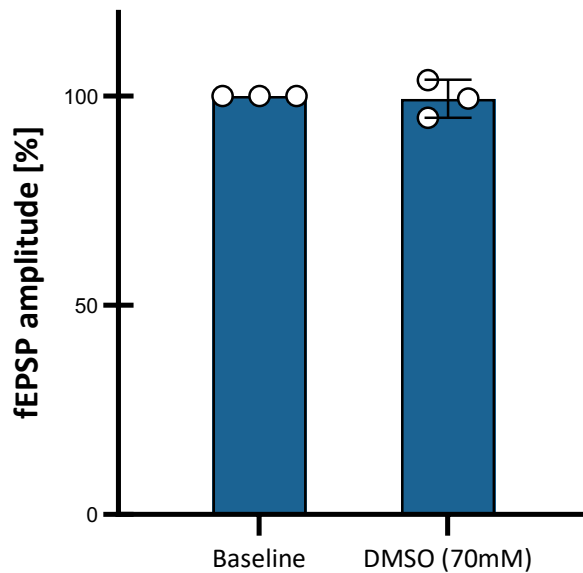
Figure 8 Synaptic transmission in hippocampal slices from seals (represented by fEPSP amplitude (mV) normalized to the baseline (%)), with perfusion of std aCSF (Baseline) and adding DMSO (70mM). Bars show mean(±SD) with actual values represented by open circles (n=4 seals).
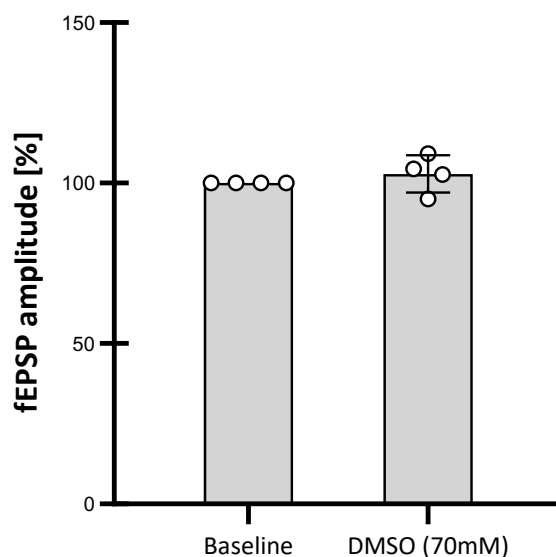
Figure 9 Synaptic transmission in hippocampal slices from mice (represented by fEPSP amplitude (mV) normalized to the baseline (%)), with perfusion of std aCSF (Baseline) and adding DMSO (70mM). Bars show mean(±SD) with actual values represented by open circles (n=3 mice).

In the experiments where CNQX (see section **2.4.2.1**) was added, clear decrease of the EPSP was observed thereby confirming that we were indeed recording synaptic signal and not an artifact (**Figure 10**).
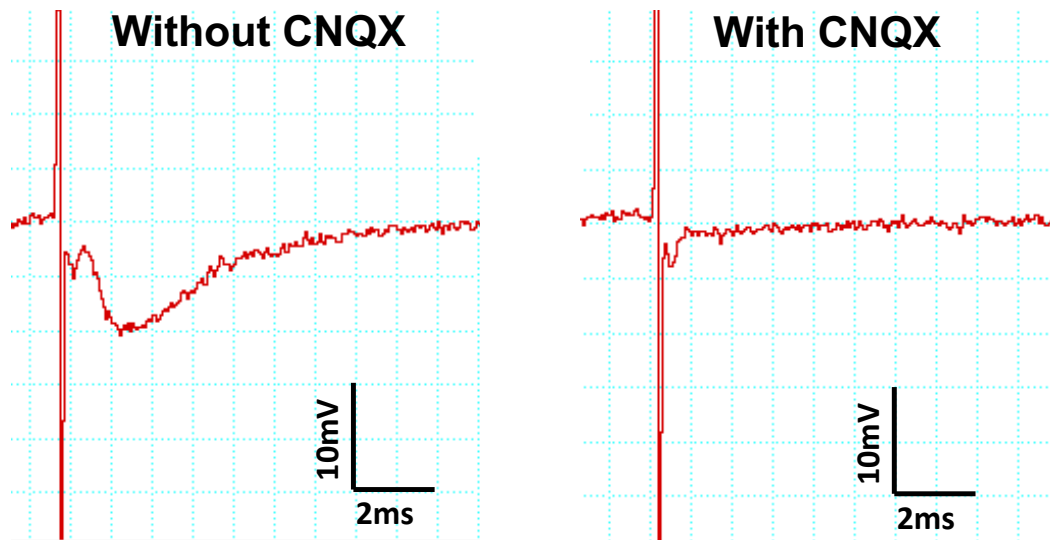
Figure 10 *Effect of AMPA-type glutamate receptor antagonist CNQX on the synaptic response (represented by fEPSP amplitude (mV) against time (ms)) in LabChart v7.0. Evoked fEPSP before and ~5 minutes after adding 25µM CNQX, proofing that the signal was synaptic and CNQX blocked it. Example signal from a mouse hippocampal slice.*

3.2.1 Lactate has suppressing effect on synaptic transmission

When exposed to lactate (20mM), fEPSP amplitude in hooded seal hippocampal slices declined 2-3 minutes after changing to lactate aCSF and started to increase again 30 seconds – 2 minutes after changing back to standard aCSF. The average fEPSP amplitude during the lactate treatment was ~78±9% of the baseline value, being significantly different (p=0.0146) when n = 4 seals (**Figure 11**). Recovery of the signal close to the baseline values (~97±11%) after rinsing with std aCSF was statistically significant as well (p=0.0335, n=4 seals).
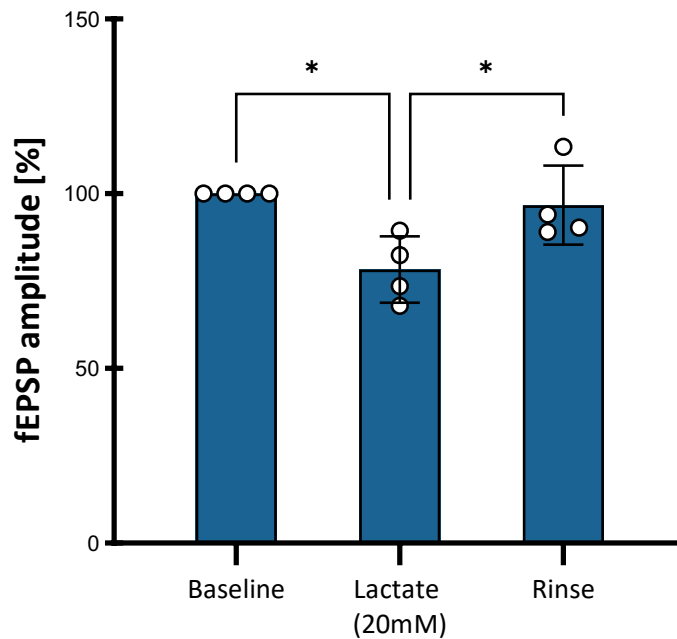
Figure 11 *Suppression of synaptic transmission in hippocampal slices from seals (represented by fEPSP amplitude (mV) normalized to the baseline (%)), by changing from perfusion with std aCSF (Baseline), to lactate aCSF (Lactate 20mM), and back to std aCSF (Rinse). Bars show mean(±SD) with actual values represented by open circles (n=4 seals). * denotes statistically significant difference (p<0.05).*

The signal amplitude of fEPSP in mouse hippocampal slices declined ~2 minutes after they were exposed to lactate aCSF (20mM). Recovery of the signal was not as strong as in hooded seal slices, but amplitude of the signal started to increase ~3 minutes after changing back to std aCSF. The average fEPSP amplitude during lactate treatment was ~54±32% of the baseline value, but it wasn't statistically significant (p=0.1102, n=3 mice) (**Figure 12**). Signal recovery after rinsing with std aCSF was average ~67±23% without significance (p=0.7847, n=3 mice).
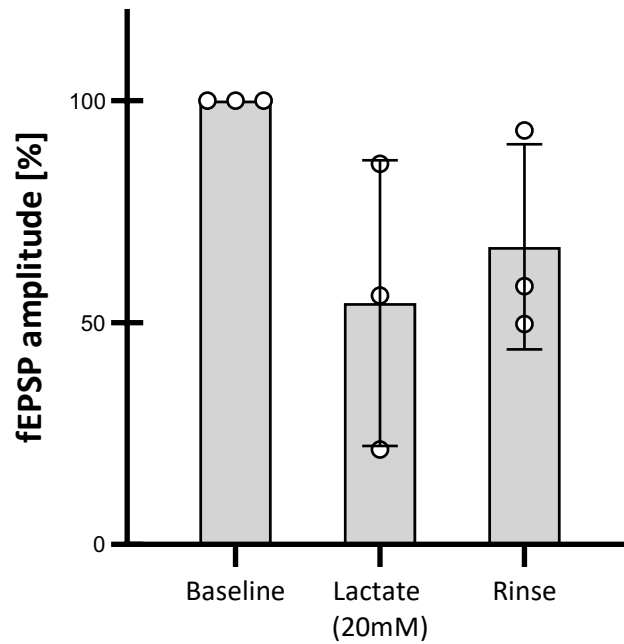
Figure 12 *Suppression of synaptic transmission in hippocampal slices from mice (represented by fEPSP amplitude (mV) normalized to the baseline (%)) by changing from perfusion with std aCSF (Baseline), to lactate aCSF (Lactate 20mM) and back to std aCSF (Rinse). Bars show mean(±SD) with actual values represented by open circles (n=3 mice). * denotes statistically significant difference (p<0.05).*

The average decrease of the fEPSP signal amplitude was significantly larger in mouse compared to seal (p=0.0446, n=4 in seals, n=3 in mice), but the signal amplitude of slices from seals recovered significantly better and closer to the baseline values after rinsing (p=0.0042, n=4 in seals, n=3 in mice) (**Figure 13**).
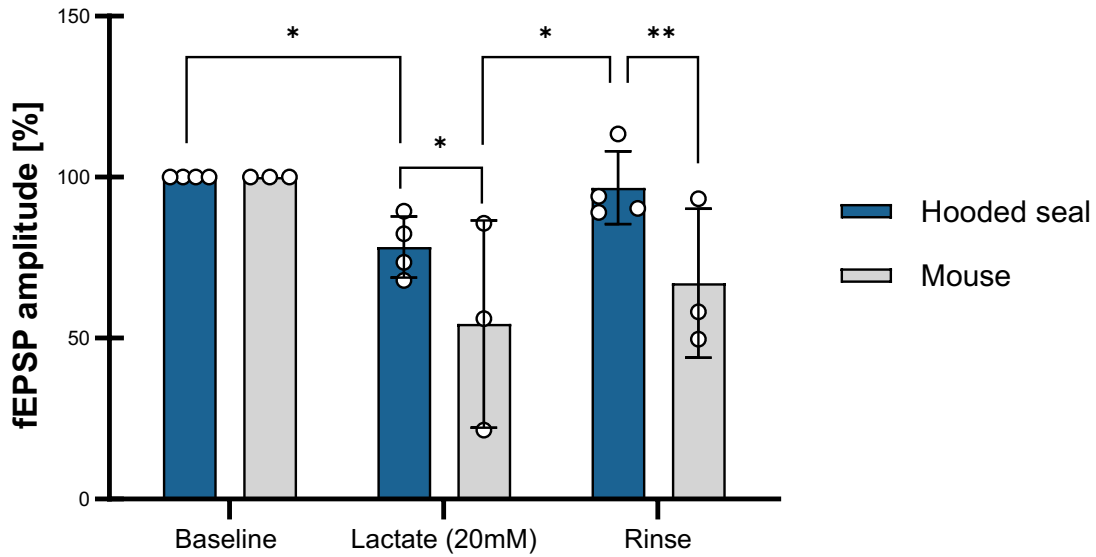
Figure 13 *Suppression of synaptic transmission in hippocampal slices from hooded seal and mouse (represented by fEPSP amplitude (mV) normalized to the baseline (%)) by changing from perfusion with std aCSF (Baseline), to lactate aCSF (Lactate 20mM) and back to std aCSF (Rinse). Bars show mean(±SD) with actual values represented by open circles (n=4 seals, n=3 mice). * denotes statistically significant difference when p<0.05, ** when p<0.01.*

3.2.2 HCAR1 agonist 3,5-DHBA suppresses synaptic transmission

Addition of the lactate receptor HCAR1 agonist 3,5-DHBA had suppressing effect on the fEPSP amplitude in hippocampal slices from hooded seal. The signal amplitude declined 2-3 minutes after addition of the agonist and the effect was similar when increasing the concentration of it. The amplitude declined to average ~88±9% in 1mM concentration of the agonist, ~78±10% in 2mM concentration and ~70±8% in 4mM concentration (**Figure 14**). The effect was significant in 4mM concentration of 3,5-DHBA (p=0.0190, n=4 seals), which is 4 times higher than previously published (1mM concentration, de Castro Abrantes et al., 2019). The amplitude increased back to average ~107±40% after rinsing the system with standard aCSF, even though this change was not deemed statistically significant (p=0.4904, n=4 seals). **Figure 15** shows a typical example recording from a seal hippocampal slice during 3,5-DHBA experiment.
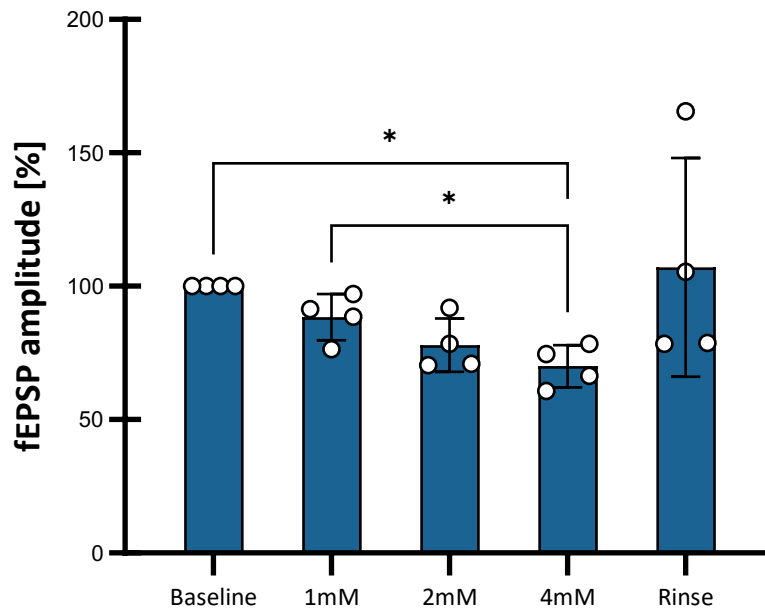
Figure 14 *Suppression of synaptic transmission in hippocampal slices from seals (represented by fEPSP amplitude (mV) normalized to the baseline (%)) with perfusion of std aCSF (Baseline) with increasing concentrations of HCAR1 agonist 3,5-DHBA (1mM, 2mM, 4mM) and after rinsing with std aCSF (Rinse). Bars show mean(±SD) with actual values represented by open circles (n=4 seals). * denotes statistically significant difference (p<0.05).*
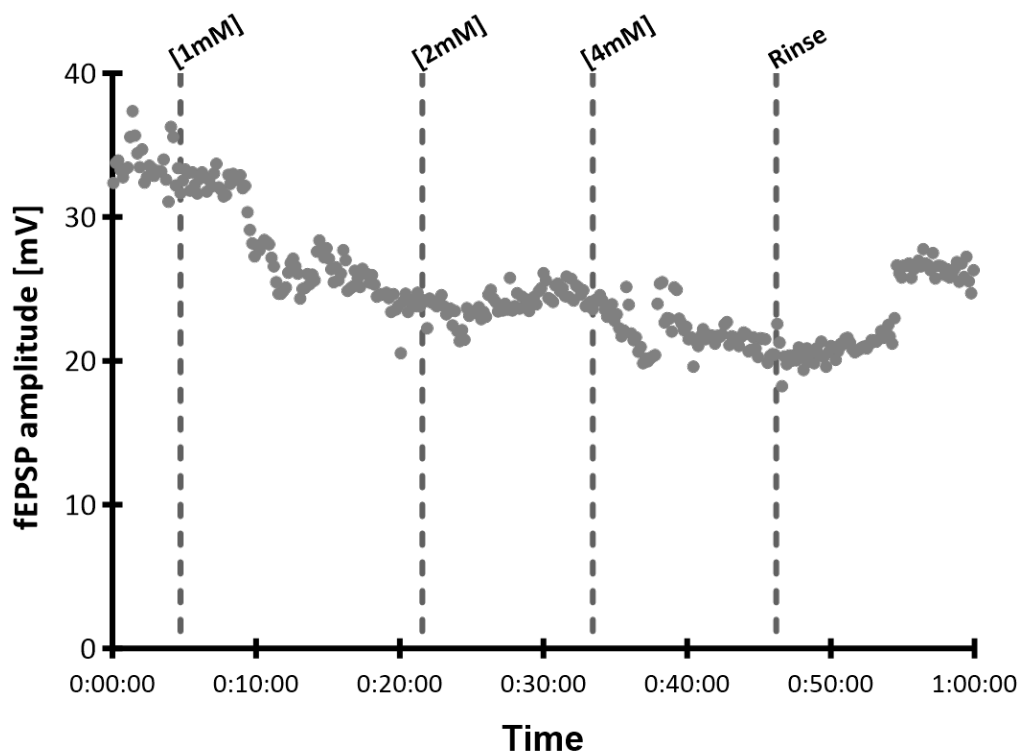
Figure 15 *Example recording of fEPSP signal amplitude (mV) from seal hippocampal slice against time (h:mm:ss) with step-wise increases in the concentration of the HCAR1 agonist 3,5-DHBA, and after rinsing with std aCSF. Data points show amplitude of individual fEPSPs and lines indicate time points for addition of the agonist/rinsing.*

The fEPSP amplitude in mouse hippocampal slices displayed a decrease 1-2 minutes after addition of the HCAR1 agonist 3,5-DHBA in aCSF, and noticeable increase ~2 minutes after rinsing the agonist away with std aCSF (**Figure 16**). Furthermore, the decrease during agonist treatment was only temporary as seen on example recording (**Figure 17**) and the amplitude started to increase again ~5 minutes after the agonist had been added, without it being rinsed from the system. In 1mM concentration of 3,5-DHBA, the signal amplitude declined to average ~92±9%, in 2mM to average ~93±11%, in 4mM to average ~82±10% and in 8mM to average ~62±14%. Difference in the amplitude of fEPSP between 1mM and 4mM concentrations was significant (p=0.0442), and between 1mM and 8mM concentrations as well (p=0.0355). The statistical analysis did not show significant difference between baseline amplitude and any concentration of the agonist, possibly due to the small sample size (n=3). However, similar short-term suppression of the amplitude as shown in the typical example recording (**Figure 17**) was evident in all the recordings in mice. The amplitude of the signal increased again after rinsing the agonist, back to a mean of ~99±28% without similar fluctuation as after adding the agonist. The increase was not statistically significant (p=0.5620).
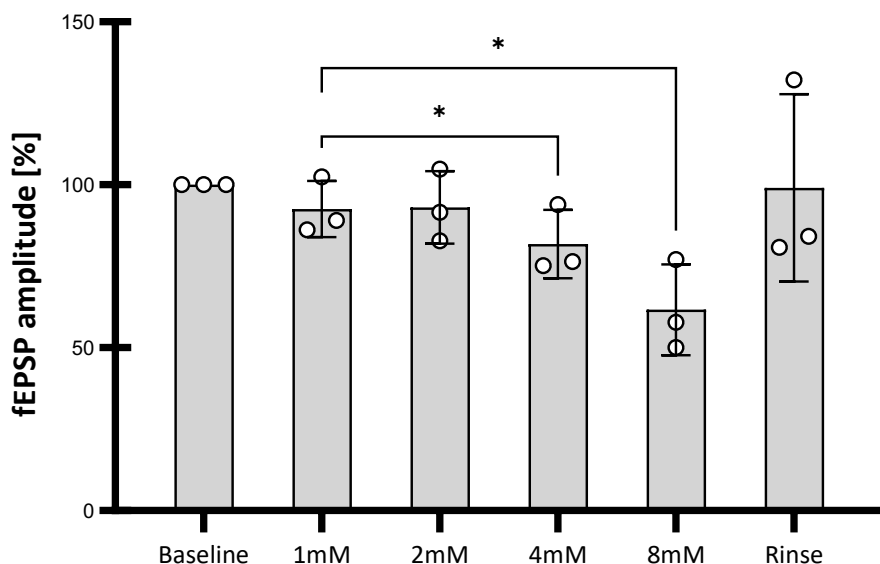
Figure 16 *Suppression of synaptic transmission in hippocampal slices from mice (represented by fEPSP amplitude (mV) normalized to the baseline (%)) with perfusion of std aCSF (Baseline) with increasing concentrations of HCAR1 agonist 3,5-DHBA (1mM, 2mM, 4mM, 8mM) and after rinsing with std aCSF (Rinse). Bars show mean(±SD) with actual values represented by open circles (n=3 mice). * denotes statistically significant difference (p<0.05).*
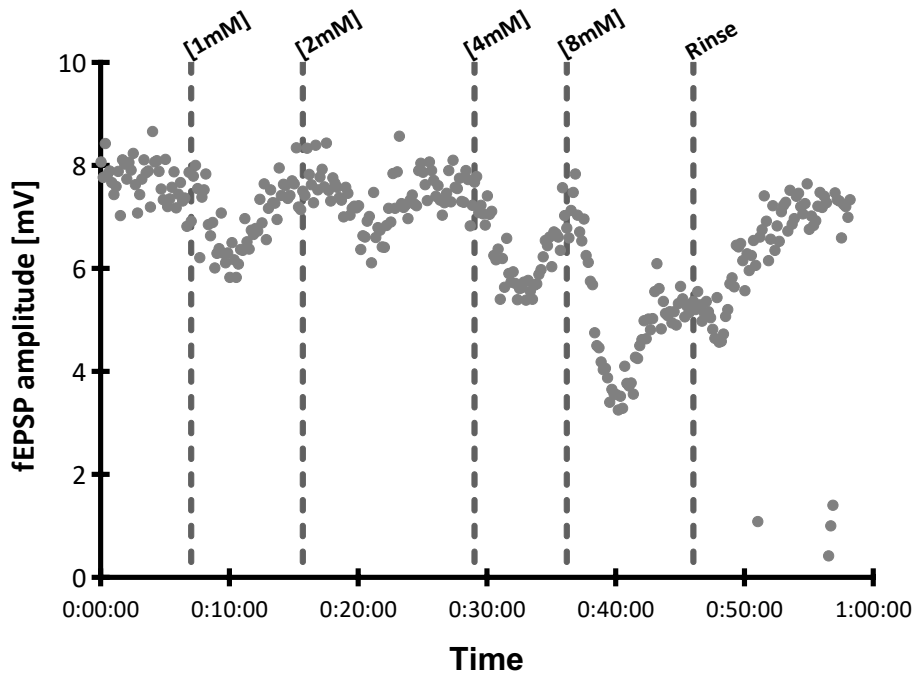
Figure 17 *Example recording of fEPSP signal amplitude (mV) from a mouse hippocampal slice against time (h:mm:ss) with step-wise increases in the concentration of the HCAR1 agonist 3,5-DHBA, and after rinsing with std aCSF. Data points show amplitude of individual fEPSPs and lines indicate time points for addition of the agonist and the time point for rinsing.*

There was no statistically significant difference in the effect of the agonist 3,5-DHBA on the amplitude between seal and mouse (1mM concentration p=0.5559, 2mM concentration p=0.1177, 4mM concentration p=0.1479) (**Figure 18**). Yet, similar temporary effect of the agonist was not observed in seals (**Figure 15**) as in mice (**Figure 17**). There was no significant difference in the signal amplitude between the species after rinsing with std aCSF (p=0.6930).
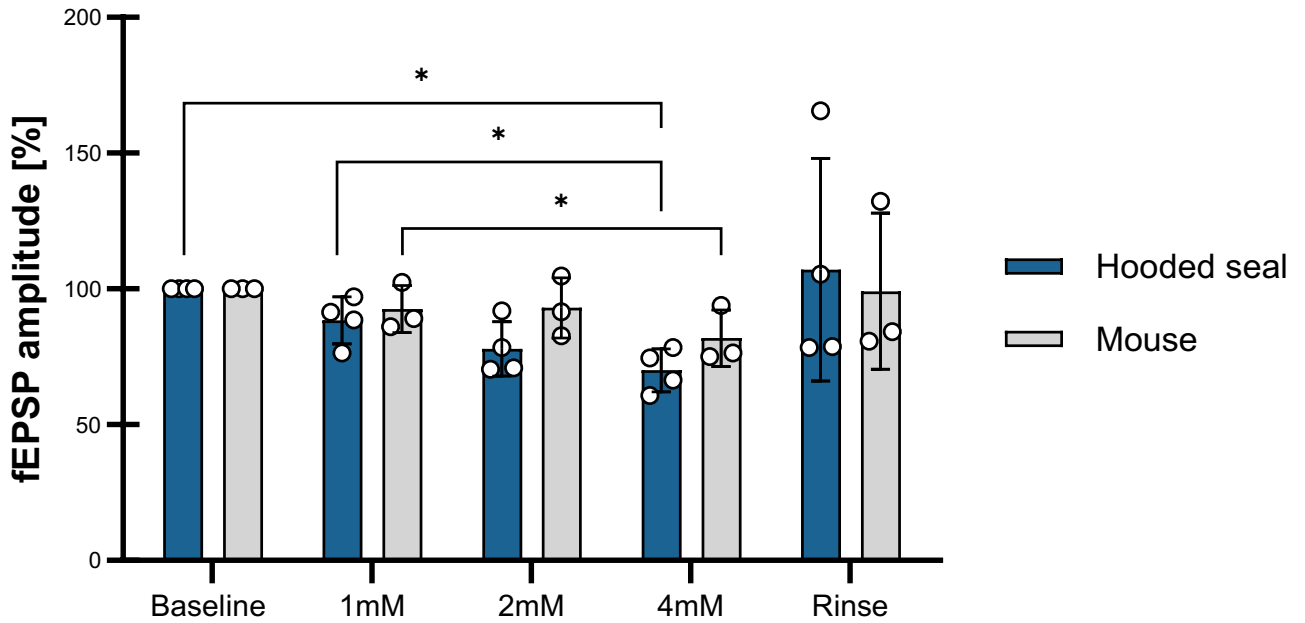
Figure 18 *Suppression of synaptic transmission in hippocampal slices from hooded seal and mouse (represented by fEPSP amplitude (mV) normalized to the baseline (%)) with perfusion of std aCSF (Baseline) with increasing concentrations of HCAR1 agonist 3,5-DHBA (1mM, 2mM, 4mM) and after rinsing with std aCSF (Rinse). Bars show mean(±SD) with actual values represented by open circles (n=4 seals, n=3 mice). * denotes statistically significant difference when p<0.05.*

The HCAR1 agonist 3,5-DHBA had no detectable effect on the fEPSP amplitude in the recordings from CA3 region of hippocampus in the hippocampal slices from mice (**Figure 19**). Amplitudes between baseline and different concentrations of the agonist were not significantly different (1mM concentration p=0.9736, 2mM concentration p=0.7453, 4mM concentration p=0.9712). Amplitude after rinsing the agonist from the system was not significantly different (p=0.4845).
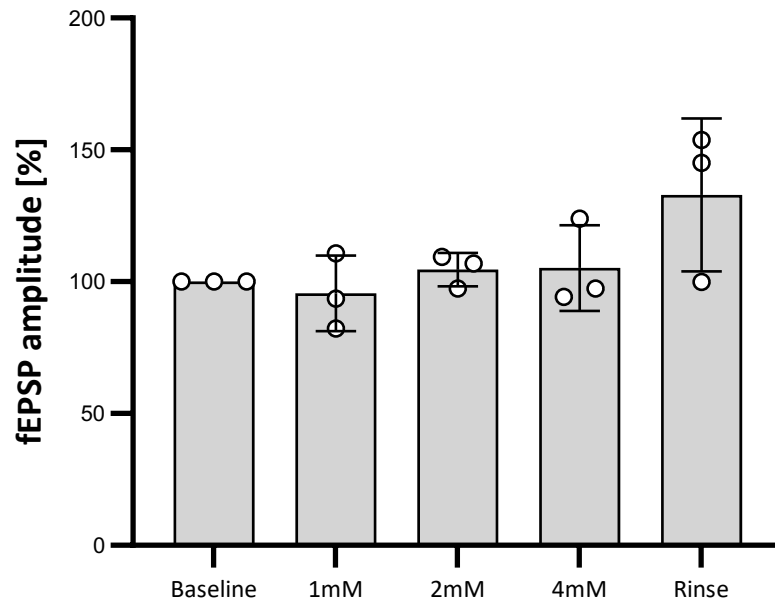
Figure 19 *Synaptic transmission in CA3 region in hippocampal slices from mice (represented by fEPSP amplitude (mV) normalized to the baseline (%)) with perfusion of std aCSF (Baseline) with increasing concentrations of HCAR1 agonist 3,5-DHBA (1mM, 2mM, 4mM) and after rinsing with std aCSF (Rinse). Bars show mean(±SD) with actual values represented by open circles (n=3 mice).*

3.2.3 No significant effect of the agonist 3Cl-HBA on the synaptic transmission

Effect of another HCAR1 receptor agonist, 3Cl-HBA was tested, but this agonist had no clear effect on the fEPSP amplitude in hippocampal slices from hooded seal. Signal amplitude declined slightly but stayed relatively close to the baseline amplitude with no significant difference in the response to any of the concentrations tested (40 µM p=0.7648, 80 µM p=0.4856, 160 µM p=0.8169, 320 µM p=0.9061) (**Figure 20**). There was no significant effect to the signal amplitude after rinsing with std aCSF either (p=0.9502), and the amplitude stayed at average ~85±35%.
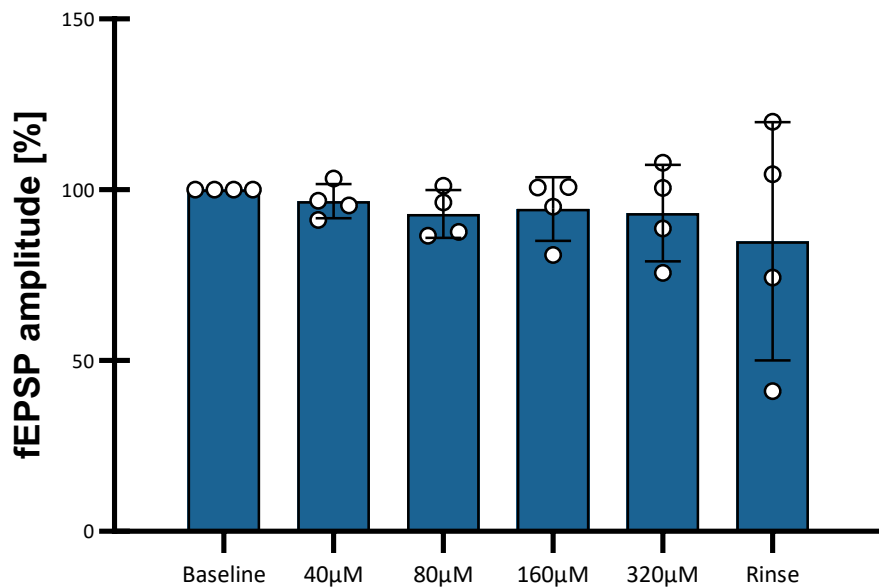
Figure 20 Synaptic transmission in hippocampal slices from seals (represented by fEPSP amplitude (mV) normalized to the baseline (%)) with perfusion of std aCSF (Baseline) with increasing concentrations of HCAR1 agonist 3Cl-HBA (40μM, 80μM, 160μM, 320μM) and after rinsing with std aCSF (Rinse). Bars show mean(±SD) with actual values represented by open circles (n=4 seals).

Addition of 3Cl-HBA didn't have any clear effect on the fEPSP amplitude in hippocampal slices from mice either. Signal first increased slightly with average ~107±10% in 40μM, but then declined somewhat at the higher concentrations with averages ~91±21% in 80μM, ~79±34% in 160μM and ~76±38% in 320μM (**Figure 21**). However, variation between signal amplitudes from different slices was large and differences from the baseline amplitude were not significant (40μM p=0.8238, 80μM p=0.9803, 160μM p=0.8538, 320μM p=0.8571). There was no significant effect to the signal amplitude after rinsing with std aCSF (p=0.9513) and the mean amplitude stayed at only ~66±19% of the baseline value.
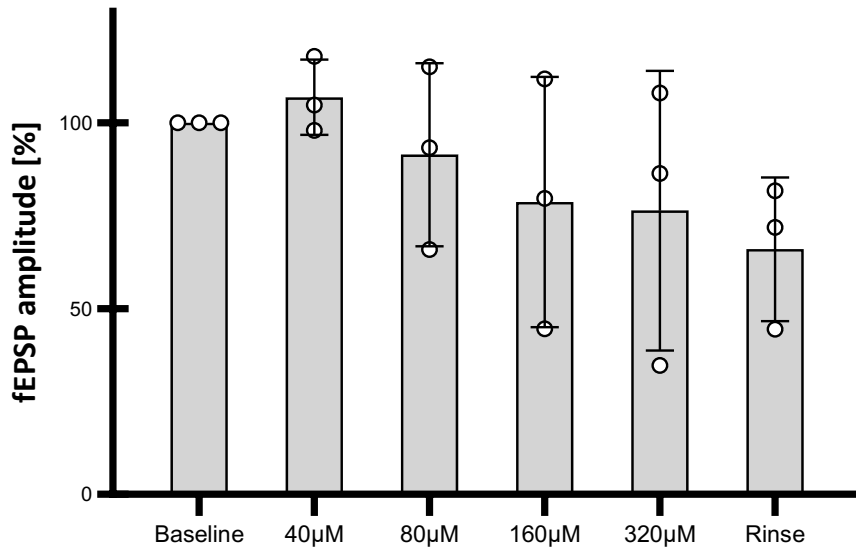
Figure 21 *Synaptic transmission in hippocampal slices from mice (represented by fEPSP amplitude (mV) normalized to the baseline (%)) with perfusion of std aCSF (Baseline) with increasing concentrations of HCAR1 agonist 3Cl-HBA (40μM, 80μM, 160μM, 320μM) and after rinsing with std aCSF (Rinse). Bars show mean(±SD) with actual values represented by open circles (n=3 mice).*

There was no statistically significant difference in the effect of the agonist 3Cl-HBA on the amplitude between seal and mouse in any of the concentrations used (40μM p=0.1340, 80μM p=0.9113, 160μM p=0.4027, 320μM p=0.4380) (**Figure 22**). There was no significant difference in the signal amplitude between the species after rinsing with std aCSF (p=0.4404).
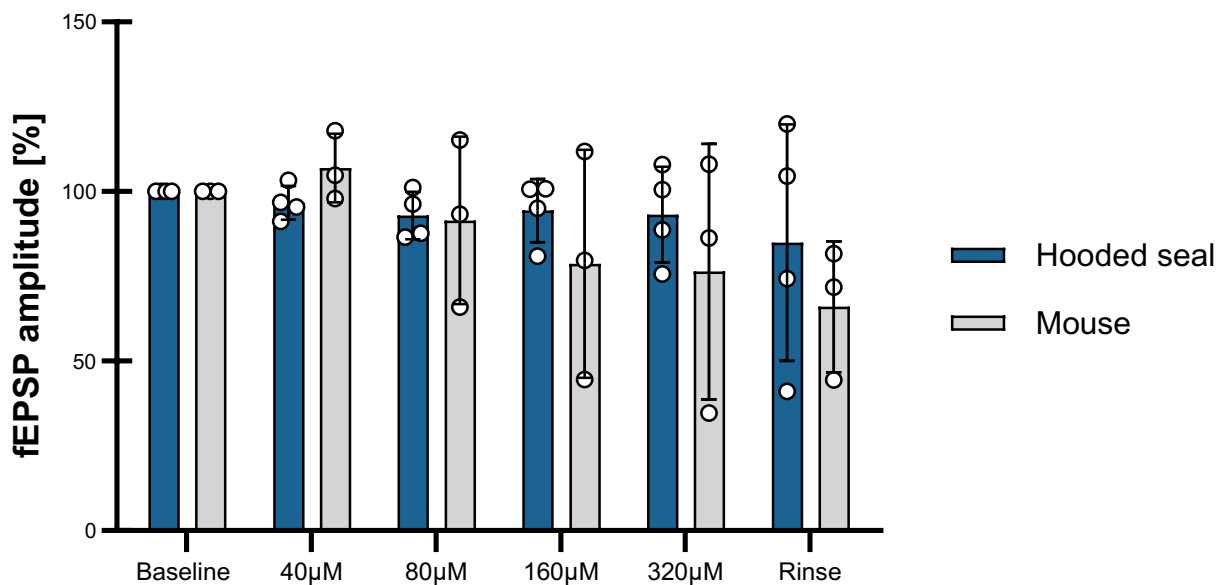
Figure 22 *Synaptic transmission in hippocampal slices from hooded seal and mouse (represented by fEPSP amplitude (mV) normalized to the baseline (%)) with perfusion of std aCSF (Baseline) with increasing concentrations of HCAR1 agonist 3Cl-HBA (40μM, 80μM, 160μM, 320μM) and after rinsing with std aCSF (Rinse). Bars show mean(±SD) with actual values represented by open circles (n=4 seals, n=3 mice).*

4 Discussion

The aim of this study was to investigate whether lactate contributes to the neural protective shutdown observed in hypoxia-tolerant hooded seal (Geiseler et al., 2016) throught activation of HCAR1 receptors. Additionally, I aimed to explore whether there are differences between hypoxia and non-hypoxia-tolerant animals in this respect, using mice as a control group. To examine potential variations in the distribution of the lactate receptor in the hippocampus, fEPSP recordings were conducted in both the CA1 and CA3 regions of mouse hippocampal slices.

The results of qPCR analysis show that HCAR1 is indeed present in the hippocampus, visual cortex and cerebellum of hooded seal (**Figure 7**). Further, the amplitude of the synaptic signal in the electrophysiological fEPSP recordings decreased in both seals (**Figure 11**) and mice (**Figure 12**) during lactate treatment. To test whether the decrease in amplitude in response to lactate was due to a change in metabolism, we also tested the non-metabolizable agonists for HCAR1. A similar decrease was observed with the 3,5-DHBA agonist (**Figure 14**, **Figure 16**), although in mice, the effect appeared to be temporary (**Figure 17**) compared to seals (**Figure 15**). These findings support the notion that lactate may act as a signaling factor to slow excitatory transmission in neurons (de Castro Abrantes et al., 2019; Briquet et al., 2022; Skwarzynska et al., 2023), including those of hooded seals. However, our experiments with the 3Cl-HBA agonist did not yield as clear results (**Figure 22**). Our findings also do not allow us to draw conclusions whether there is a difference in the effect of the lactate between the CA1 and CA3 regions in mice (**Figure 19**).

4.1 HCAR is expressed in the hippocampus of the hooded seal

The results from qPCR analysis revealed expression of HCAR1 mRNA in the hippocampus, visual cortex and cerebellum of hooded seals (**Figure 7**). HCAR1 has been reported to be localized in neurons of mice (Bozzo et al., 2013; Lauritzen et al., 2014; de Castro Abrantes et al., 2019). Moreover, HCAR1 mRNA has been demonstrated to be distributed throughout the brain, suggesting the signaling effects of lactate through the receptor activation in widespread regions of the CNS. This implies that the effects of lactate link synaptic function, energy metabolism and cerebral blood flow together (Morland et al., 2015). Given the presence of

HCAR1 in several regions of the CNS of the hooded seal, a similar contribution and connection seems to exist in the hooded seal, potentially linking lactate to a neural protective shutdown in this species (Ramirez et al., 2007; Geiseler et al., 2016).

4.2 Lactate suppresses the amplitude of fEPSP

Numerous prior studies have demonstrated that the activation of the HCAR1 receptor downmodulates neuronal activity (Herrera-Lopez and Galvan, 2020; de Castro Abrantes et al., 2019; Briquet et al., 2022; Skwarzynska et al., 2023), by means of mechanisms that are discussed below. This decrease has been observed in both human and rodent brain (Briquet et al., 2022). Since the majority of these studies have recorded spontaneous activity and primarily investigated the impact of HCAR1 activation on its frequency (de Castro Abrantes et al., 2019; Briquet et al., 2022; Skwarzynska et al., 2023), it is challenging to compare the percentage of decrease to our results. Some decrease in amplitude during spontaneous activity was reported as well (de Castro Abrantes et al., 2019). The overall decreasing effect on synaptic activity via HCAR1 activation in our results with evoked activity (fEPSP) aligns with the previous findings. Both lactate (**Figure 11**, **Figure 12**) and non-metabolizable specific HCAR1-agonist 3,5-DHBA (**Figure 14**, **Figure 16**) reduced the amplitude of fEPSP both in seal and mouse (**Figure 13**, **Figure 18**), although in mice, these results did not exhibit statistically significant changes compared to the baseline. Therefore, HCAR1 activation also appear to diminish fEPSP amplitude, even though 3Cl-HBA agonist did not yield as clear results (**Figure 20**, **Figure 21**, **Figure 22**).

During hypoxia, neural energy production switches to anaerobic glycolysis with lactate as the end product. In non-hypoxia tolerant animals, the resulting insufficient ATP-supply leads to a so called excitotoxic cascade, where the loss of stable membrane potential leads to excessive glutamate release and Ca^{2+} influx, which over activates the enzyme systems and results in damage of cell components (Dirnagl et al., 1999; Drew et al., 2004). As previously discussed, in seals such an excessive neuronal activity is presumably not present during hypoxia (Folkow et al., 2008; Geiseler et al., 2016), but they may exhibit high post-dive levels of lactate up to 14 mM in the blood plasma (Scholander 1940; Kooyman et al., 1980; Kooyman et al., 1983). In addition, even during resting conditions 20-25% of the utilized blood glucose was released as lactate, when in rats it was only 5-15% (Murphy et al., 1980). This

association between the higher-than-normal levels of lactate caused by anaerobic metabolism during diving, and the presence of lactate signaling in hooded seal strongly suggests that lactate contributes to the neural protective shutdown observed in hooded seals.

Why does the synaptic activity decrease when HCAR1 is activated? The detailed mechanisms of HCAR1 activation remain unclear, but it has been shown to decrease the neural activity by decreasing the frequency of spontaneous post-synaptic activity (de Castro Abrantes et al., 2019; Briquet et al., 2022; Skwarzynska et al., 2023) and by inducing a decrease in neuronal Ca^{2+} spiking activity (Bozzo et al., 2013; Briquet et al., 2022). These depressing effects have been observed in cultured cells as well as in networks of cells, such as cultured primary cortical neurons (Briquet et al., 2022), and in rat CA3 pyramidal neurons (Herrera-Lopez and Galvan, 2020). Additionally, HCAR1 has also been shown to hyperpolarize CA1 pyramidal neurons (Skwarzynska et al., 2023).

One aspect in the role of the receptor is an overall feed-back function against excessive activity (Morland 2015). HCAR1 has been suggested to convey presynaptic control of spontaneous neurotransmitter release (Briquet et al., 2022; de Castro Abrantes et al., 2019; Skwarzynska et al., 2023). Indeed, the frequency of spontaneous excitatory post-synaptic currents decreased during HCAR1 activation in WT (wild-type) mice, but not in multiple different KO (knockout) mice (de Castro Abrantes et al., 2019; Skwarzynska et al., 2023). This suggests a diminished presynaptic release of excitatory neurotransmitters such as glutamate, which may also explain the observed decrease in the amplitude of excitatory post-synaptic potentials during HCAR1 activation in our results. If fewer Ca^{2+} ions flow into the presynaptic neuron, fewer vesicles containing neurotransmitters such as glutamate will be released. As a result, there is less activation of ion channels on the postsynaptic neuron, leading to decrease in positive ions flowing into the cell and triggering post-synaptic potential (Hill et al., 2018).

The exact location of the HCAR1 receptor in the cells and its specific signaling pathway remain unclear, but there is an indication that it is concentrated on post-synaptic neurons (Morland et al., 2015). In this context, it could be suggested that the effect of the receptor could be explained by hyperpolarization of the postsynaptic membrane. However, Skwarzynska et al. (2023) demonstrated that the activation of the HCAR1 did not have an effect on the spontaneous inhibitory post-synaptic current, thus not causing hyperpolarization.

As a G-protein coupled receptor, the activation of HCAR1 has been shown to lead to the downregulation of cAMP (Lauritzen et al., 2014). A study by de Castro Abrantes et al. (2019) suggested that the adenylyl cyclase (AC) – cAMP – protein kinase A (PKA) pathway is involved in the HCAR1 downmodulation of neuronal activity. They demonstrated this by pharmacologically manipulating the downstream factors (AC, cAMP, PKA) of the pathway together with HCAR1 activation, showing that this affected the outcome. This collectively indicates that HCAR1 action on neuronal spiking activity involves inhibition of the AC, causing a decrease in cAMP levels which will turn of PKA activity. Furthermore, HCAR1 appears to interact with other GPCRs such as adenosine receptor A1, GABA$_B$ receptor and α_{2A} -adrenoreceptor through activation of its G$_\alpha$ and G$_{\beta\gamma}$ subunits (de Castro Abrantes et al., 2019). These interactions add a higher level of complexity to the functional outcomes of HCAR1 activation. Also, adenosine and GABA$_B$ receptors typically have hyperpolarizing effects (Rudolphi et al., 1992; Daroff et al., 2014) further suggesting a post-synaptic inhibition (hyperpolarization) effect of HCAR1.

Based on known effects of HCAR1 in other tissues, the downregulation of cAMP by HCAR1 activation has been suggested to have glucose-saving effects due to the depressed synaptic activity in brain cells, potentially preventing damage in hypoxic conditions (Morland et al., 2015).

Our results do not allow us to conclude whether there is a distinction in the effect on the synaptic transmission with HCAR1 activation between CA1 and CA3 (**Figure 19**) regions of the mouse hippocampus, or on the specific mode of action in the hooded seal preparation. Previous research indicates that HCAR1 activation causes neuromodulation in the DG of the hippocampus in mice and rats, and it appears to have presynaptic action on glutamatergic neurotransmission provided by mossy fibers, which are key players in the hippocampal excitatory circuitry (Briquet et al., 2022). In the CA1 region, HCAR1 activation shows a clear decreasing effect on neuronal excitability as well (Herrera-Lopez and Galvan, 2018; Skwarzynska et al., 2023).

4.3 Differences between the species

Both mice and seal exhibited attenuated synaptic transmission during HCAR1 activation. However, in mice, the effect of 3,5-DHBA agonist showed a temporal effect (**Figure 17**),

whereas in seals the effect appeared to be more cumulative (**Figure 15**). HCAR1 stimulation by lactate has been described to promote internalization of the receptor, involving trafficking of it between the plasma membrane and intracellular stores (Liu et al., 2009; Morland et al., 2015), a phenomenon observed also in other GPCRs (Vistein and Puthenveedu, 2013; Weinberg and Puthenveedu, 2020). Since seals seem to exhibit a more cumulative effect on the HCAR1 activation with 3,5-DHBA, this might suggest differences in the mechanisms of the receptor, or possibly trafficking of it in the seals, since this kind of impression of the trafficking was not as noticeable in seals as in mice.

As previously mentioned, HCAR1 has been demonstrated to decrease Ca^{2+} spiking in rodents (Bozzo et al., 2013; Briquet et al., 2022), and it has been shown to alter the paired-pulse ratio of evoked EPSCs in HCAR1 WT mice, but not in KO mice (Skwarzynska et al., 2023). This is interesting especially in the context of the attenuated PPF in hooded seal. As discussed earlier (see section 1.4.2), this attenuated paired-pulse facilitation (PPF) in hooded seal may potentially indicate a modification in presynaptic Ca^{2+} regulation, aiming to mitigate the detrimental effects of excessive Ca^{2+} influx (Geiseler et al., 2016). This implies that the HCAR1 activation – that possibly has presynaptic effects – could be linked to the observed attenuated PPF during the neural protective shutdown in hooded seals, since HCAR1 has been shown to decrease Ca^{2+} spiking (Bozzo et al., 2013; Briquet et al., 2022).

Synaptic transmission in seal neurons exhibited significant recovery after the lactate treatment (**Figure 11**) compared to mice (**Figure 12**, **Figure 13**). Reason behind the apparently less complete recovery of mice neurons could be the metabolic aspects. Lactate can be beneficial for the brain, but only up to a certain concentration (Bergersen, 2015). Post-dive plasma levels of lactate from 14 mM to 25 mM have been recorded in seals (Scholander 1940; Kooyman et al., 1980; Kooyman et al., 1983) and the hooded seal brain has been shown to tolerate lactate levels up to 20 mM. In contrast, in mice, neuronal activity rapidly diminished with increasing lactate levels (Czech-Damal et al., 2014). Notably, seal neurons also possess higher intrinsic energy stores with glycogen stores approximately three times larger than in mouse brain (Czech-Damal et al., 2014). This could suggest that the mice neurons may have run out of energy stores during the experiment, and therefore did not recover. However, due to the small sample size, further experiments are necessary to clarify this observation.

4.4 Functional implications

Possible factors contributing to the shutdown response in seals during diving is altered neural metabolism together with other mechanisms. Reversed ANLS has been suggested on seals, and hypothesis is that due to the localization of mitochondria and neuroglobin in astrocytes, oxidative metabolism seems to be located primarily in astrocytes instead of neurons in seals (Mitz et al., 2009, Schneuer et al., 2012). The benefit of this would be that it reduces the reliance of seal neurons on oxygen and prevents them from experiencing oxidative stress caused by mitochondrial activity (Turrens, 2003; Mitz et al., 2009). Therefore, while seals are diving, lactate will be produced by neural activity and the lactate will have a self-stimulating effect on the neurons by activating HCAR1 receptors in several brain regions of seals. Activation of HCAR1 will then suppress the synaptic transmission and neural activity overall, resulting in energy savings for the seal brain during diving.

Activation of HCAR1 has been shown to increase brain capillary density in mice (Morland et al., 2017) which is another advantage during diving to enhance oxygen supply to the brain. Indeed, it has been indicated that hooded seals have a higher capillary density than mammals that are the same size (Ludvigsen, 2010).

4.5 Variation in the response between different agonists

The non-metabolic HCAR1 agonist, 3Cl-HBA, did not exhibit a significant effect on the synaptic response any species (**Figure 22**). Although there was considerable variation in the results, the amplitude of the synaptic signal tended to decrease both in mice (**Figure 21**) and seals (**Figure 20**). Overall, other agonists for HCAR1, lactate and 3,5-DHBA, demonstrated a decrease. Following rinsing, in experiments with lactate (**Figure 13**) and non-metabolic 3,5-DHBA (**Figure 18**), both showed more recovery of the signal amplitude, to levels close to the baseline values, than was the case after adding 3Cl-HBA in increasing levels.

3Cl-HBA is a more recent agonist for HCAR1, and it has higher affinity in mice compared to 3,5-DHBA (de Castro Abrantes et al., 2019). In previous research using 3Cl-HBA, the frequency of neuronal activity showed an increase after the agonist was washed out from the neurons from WT mice. Although the signal amplitude also did show some increase,

it was not statistically significant compared to the amplitude during agonist treatment (de Castro Abrantes et al., 2019). The concentration used in their study (40 µM) was much lower than ours (320 µM). Therefore, the lack of recovery of signal amplitude after rinsing could be connected to the high concentration, suggesting that either it was challenging to wash the agonist away and we would have needed to wait much longer for the recovery, or the agonist may have had a toxic effect at such a high concentration.

3Cl-HBA has been used in higher doses as well (100 µM, Skwarzynska et al., 2023), however these experiments did not involve attempting to wash the agonist away from the tissue. In the experiment conducted by de Castro Abrantes et al. (2019) all the drugs were diluted in CO_2/bicarbonate buffered solution, whereas in our experiments 3Cl-HBA was diluted with DMSO - a widely used solvent used in experiments without causing any significant damage (Szmant, 1975). Control experiments, using three slices from one seal and slices from four different mice were used, indicated no observable effect of DMSO on the signal (**Figure 8**, **Figure 9**).

4.6 Methodological considerations

Adding 25 µM CNQX (see section **2.4.2.1**) to the system resulted in the disappearance of the synaptic signal (**Figure 10**). This serves as a proof that we were indeed recording synaptic signal (Blake et al., 1988), consistent with previously experiments with the same set-up that was used by Geiseler et al. (2016).

Some recorded experiments proved to be unusable during further analyses of signals, which partially explains the low sample size in mice. Experiments on CA3 region were particularly challenging, with the signal being relatively easy to find, but often unstable and disappearing quickly. CA3 region seems to be more vulnerable to mechanical stress (Mao et al., 2013), in this case caused by cutting and moving the slices, which may partially explain these challenges. The mouse hippocampus is also much smaller, providing much less tissue for sampling compared to seals. Since hippocampal slices from seals exhibit higher tolerance (Geiseler et al., 2016), sampling can continue for a longer duration. In contrast, in mice, the slices may cease to respond to stimulation, or the signal may not remain stable for an extended period.

No antagonist experiments were performed to try to prevent HCAR1 activation, since none seem to exist, and we did not have access to HCAR1-knockout mice.

4.7 Future perspectives

Given that HCAR1 activation has been demonstrated to modify the paired pulse-ratio of evoked potentials in mice (Skwarzynska et al., 2023), analyzing the PPF experiments conducted (but not yet analyzed in this project) could provide additional insights into the role of HCAR1 in hooded seals. As HCAR1 has been suggested to have a presynaptic effect (de Castro Abrantes et al., 2019; Briquet et al., 2022; Skwarzynska et al., 2023), PPF experiments on seals might uncover a potential link between HCAR1 activation and the attenuated PPF in hooded seals, as reduced PPF has been proposed to result from altered presynaptic Ca^{2+} regulation (Larson and Park, 2009; Geiseler et al., 2016). To investigate further the Ca^{2+} signaling in seals, calcium imaging could be a method to use since it could be a way to measure the Ca^{2+} status of the neurons. Regarding HCAR1, many (de Castro Abrantes et al., 2019; Briquet et al., 2022; Skwarzynska et al., 2023) have used this technique to investigate the effect of HCAR1 activation on rodents. Therefore, it could be attempted to apply on seals as well.

Originally, experiments on HCAR1 activation in hypoxic conditions in mice were planned as part of this project, but they proved challenging, primarily due to the variations in synaptic amplitude depending on recorded slice. If limitations in this aspect could be solved, it would be interesting to investigate whether HCAR1 activation improves the recovery of mouse neurons from hypoxia. Generating additional data is also necessary to examine possible differences between the CA1 and CA3 regions of the hippocampus in relation to HCAR1.

To further investigate potential causes for the differences observed between mice and seals, I would suggest additional experiments to be done on mice. This would clarify the effects that remained unclear due to low sample size in this project. Such additional experiments would have the potential to reveal the effects of both lactate and the non-metabolic agonist 3,5-DHBA more clearly. Moreover, experiments involving the higher affinity 3Cl-HBA at lower concentrations could be performed to explore if this would produce more clear response and

rule out potential technical issues such as toxic effects or excessive high concentration to wash-out.

Exploring downstream effects of the receptor in hooded seal could provide valuable insights, although the availability of fresh tissue may pose challenges. de Castro Abrantes et al. (2019) investigated the intracellular signaling pathways of HCAR1 by pharmacologically manipulating each component (AC – cAMP – PKA) individually, along with HCAR1 activation. Similar manipulation experiments, along with calcium imaging, could be applied on seals to investigate whether there are any differences compared to rodents.

Nevertheless, experiments that were conducted – to optimize the use of the animals - but not discussed here due to them being beyond the scope of my project, are likely to provide more insights in the neural protective shutdown of hooded seal and the role of lactate in it. These experiments include the fEPSP experiments related to adenosine and K_{ATP}-channels, as well as incubation experiments under hypoxic conditions and subsequent RNAseq analyses.

5   Conclusion

To conclude, the results of this study demonstrate the presence of the lactate receptor HCAR1 in the central nervous system of deep-diving, hypoxia-tolerant hooded seals and suggest that it has a functional role in it. Activation of the receptor, both with lactate and its non-metabolic agonist 3,5-DHBA, suppresses the amplitude of the synaptic signal in both hooded seals and mice. However, differences in the metabolic aspects and the cumulative strength of the effect between the two species exist. This suggests that lactate may play a role in the neural protective shutdown of hooded seal during deep and long dives when they experience hypoxia, and lactate accumulates in high concentrations in their circulation. Since HCAR1 has been suggested to have presynaptic effects, the receptor might specifically contribute to the attenuated paired pulse facilitation in hooded seals, a hypothesis that possibly could be tested by further data analysis of the existing data set (in which PPT experiments were conducted). This may contribute to a better understanding of the mechanisms underlying the neural protective shutdown in hooded seals. Furthermore, comparing these mechanisms with those in non-hypoxia tolerant animals, may reveal key elements in preventing neuronal excitability during hypoxic conditions – knowledge that may be transferrable to clinical problems, as suggested by Ramirez and colleagues (2007).

References

Alle, H., Roth, A., & Geiger, J. R. (2009). Energy-efficient action potentials in hippocampal mossy fibers. *Science*, *325*(5946), 1405-1408.

Andersen, J. M., Skern-Mauritzen, M., Boehme, L., Wiersma, Y. F., Rosing-Asvid, A., Hammill, M. O., & Stenson, G. B. (2013). Investigating annual diving behaviour by hooded seals (Cystophora cristata) within the Northwest Atlantic Ocean. *PLoS One*, *8*(11), e80438.

Ballanyi, K. (2004). Protective role of neuronal KATP channels in brain hypoxia. *Journal of Experimental Biology*, *207*(18), 3201-3212.

Bergersen, L. H. (2007). Is lactate food for neurons? Comparison of monocarboxylate transporter subtypes in brain and muscle. *Neuroscience*, *145*(1), 11-19.

Bergersen, L. H. (2015). Lactate transport and signaling in the brain: potential therapeutic targets and roles in body—Brain interaction. *Journal of Cerebral Blood Flow & Metabolism*, *35*(2), 176-185.

Bickler, P. E., Gallego, S. M., & Hansen, B. M. (1993). Developmental changes in intracellular calcium regulation in rat cerebral cortex during hypoxia. *Journal of Cerebral Blood Flow & Metabolism*, *13*(5), 811-819.

Blake, J. F., Brown, M. W., & Collingridge, G. L. (1988). CNQX blocks acidic amino acid induced depolarizations and synaptic components mediated by non-NMDA receptors in rat hippocampal slices. *Neuroscience letters*, *89*(2), 182-186.

Blix, A. S. (1987). Diving responses: fact or fiction. *Physiology*, *2*(2), 64–66.

Blix A.S. (2005) Arctic animals. Tapir Academic press, Trondheim.

Blix, A. S. (2018). Adaptations to deep and prolonged diving in phocid seals. *Journal of Experimental Biology*, *221*(12), jeb182972.

Bowen, W. D., Oftedal, O. T., & Boness, D. J. (1985). Birth to weaning in 4 days: remarkable growth in the hooded seal, Cystophora cristata. *Canadian Journal of Zoology*, *63*(12), 2841–2846.

Bozzo, L., Puyal, J., & Chatton, J. Y. (2013). Lactate modulates the activity of primary cortical neurons through a receptor-mediated pathway. *PloS one*, *8*(8), e71721.

Briquet, M., Rocher, A. B., Alessandri, M., Rosenberg, N., de Castro Abrantes, H., Wellbourne-Wood, J., ... & Chatton, J. Y. (2022). Activation of lactate receptor HCAR1 down-modulates neuronal activity in rodent and human brain tissue. *Journal of Cerebral Blood Flow & Metabolism*, *42*(9), 1650-1665.

Brown, A. M., & Ransom, B. R. (2007). Astrocyte glycogen and brain energy metabolism. *Glia*, *55*(12), 1263-1271.

Burmester, T., Weich, B., Reinhardt, S., & Hankeln, T. (2000). A vertebrate globin expressed in the brain. *nature*, *407*(6803), 520-523.

Burns, J. M., Blix, A. S., & Folkow, L. P. (2000). Physiological constraint and diving ability: a test in hooded seals, Cystophora cristata. In *Faseb Journal* 14(4), A440-A440.

Burns, J. M., Lestyk, K. C., Folkow, L. P., Hammill, M. O., & Blix, A. S. (2007). Size and distribution of oxygen stores in harp and hooded seals from birth to maturity. *Journal of Comparative Physiology B*, *177*(6), 687–700.

Cabanac, A. J., Messelt, E. B., Folkow, L. P., & Blix, A. S. (1999). The structure and blood-storing function of the spleen of the hooded seal (Cystophora cristata). *Journal of Zoology*, *248*(1), 75–81.

Caputa, M., Folkow, L., & Blix, A. S. (1998). Rapid brain cooling in diving ducks. *American Journal of Physiology-Regulatory, Integrative and Comparative Physiology*, *275*(2), R363-R371.

Choi, D. W. (1988). Glutamate neurotoxicity and diseases of the nervous system. *Neuron*, *1*(8), 623-634.

Clarke, D. D., Sokoloff L. (1999). Circulation and energy metabolism of the brain. *Basic neurochemistry: Molecular, cellular, and medical aspects*.

Clausen, G., & Ersland, A. (1969). The respiratory properties of the blood of the bladdernose seal (Cystophora cristata). *Respiration Physiology*, *7*(1), 1-6.

Cunha, R. A. (2005). Neuroprotection by adenosine in the brain: from A 1 receptor activation to A 2A receptor blockade. *Purinergic signalling*, *1*, 111-134.

Czech-Damal, N. U., Geiseler, S. J., Hoff, M. L. M., Schliep, R., Ramirez, J. M., Folkow, L. P., & Burmester, T. (2014). The role of glycogen, glucose and lactate in neuronal activity during hypoxia in the hooded seal (Cystophora cristata) brain. *Neuroscience*, *275*, 374-383.

Daroff, R. B., & Aminoff, M. J. (2014). Hippocampus. *Encyclopedia of the neurological sciences*. Academic press. 566-570.

de Castro Abrantes, H., Briquet, M., Schmuziger, C., Restivo, L., Puyal, J., Rosenberg, N., ... & Chatton, J. Y. (2019). The lactate receptor HCAR1 modulates neuronal network activity through the activation of Gα and Gβγ subunits. *Journal of neuroscience*, *39*(23), 4422-4433.

Dirnagl, U., Iadecola, C., & Moskowitz, M. A. (1999). Pathobiology of ischaemic stroke: an integrated view. *Trends in neurosciences*, *22*(9), 391-397.

Drew, K. L., Zuckerman, J. A., Shenk, P. E., Bogren, L. K., Jinka, T. R., & Moore, J. T. (2013). Hibernation: a natural model of tolerance to cerebral ischemia/reperfusion. *Innate Tolerance in the CNS: Translational Neuroprotection by Pre-and Post-Conditioning*, 37-50.

Elsner, R. (1995). Splenic oxygen storage and blood viscosity in seals. *Marine mammal science*, *11*(1), 93–96.

Erecińska, M., & Silver, I. A. (1989). ATP and brain function. *Journal of Cerebral Blood Flow & Metabolism*, *9*(1), 2-19.

Erecińska, M., & Silver, I. A. (1994). Ions and energy in mammalian brain. *Progress in neurobiology*, *43*(1), 37-71.

Erecińska, M., & Silver, I. A. (2001). Tissue oxygen tension and brain sensitivity to hypoxia. *Respiration physiology*, *128*(3), 263-276.

Fillenz, M. (2005). The role of lactate in brain metabolism. *Neurochemistry international*, *47*(6), 413-417.

Folkow, L. P., & Blix, A. S. (1995). Distribution and diving behaviour of hooded seals. *Developments in Marine Biology*, *4*, 193–202.

Folkow, L. P., & Blix, A. S. (1999). Diving behaviour of hooded seals (Cystophora cristata) in the Greenland and Norwegian Seas. *Polar Biology*, *22*, 61-74.

Folkow, L. P., Mårtensson, P. E., & Blix, A. S. (1996). Annual distribution of hooded seals (Cystophora cristata) in the Greenland and Norwegian Seas. *Polar Biology*, *16*, 179-189.

Folkow, L. P., Ramirez, J. M., Ludvigsen, S., Ramirez, N., & Blix, A. S. (2008). Remarkable neuronal hypoxia tolerance in the deep-diving adult hooded seal (Cystophora cristata). *Neuroscience letters*, *446*(2-3), 147-150.

Fujimura, N., Tanaka, E., Yamamoto, S., Shigemori, M., & Higashi, H. (1997). Contribution of ATP-sensitive potassium channels to hypoxic hyperpolarization in rat hippocampal CA1 neurons in vitro. *Journal of Neurophysiology*, *77*(1), 378-385.

Ge, H., Weiszmann, J., Reagan, J. D., Gupte, J., Baribault, H., Gyuris, T., ... & Li, Y. (2008). Elucidation of signaling and functional activities of an orphan GPCR, GPR81. *Journal of lipid research*, *49*(4), 797-803.

Geiseler, S. J., Ludvigsen, S., & Folkow, L. P. (2015). KATP-channels play a minor role in the protective hypoxic shut-down of cerebellar activity in eider ducks (Somateria mollissima). *Neuroscience*, *284*, 751-758.

Geiseler, S. (2016). Breathtaking brains Intrinsic neural adaptations to hypoxia.

Geiseler, S. J., Larson, J., & Folkow, L. P. (2016). Synaptic transmission despite severe hypoxia in hippocampal slices of the deep-diving hooded seal. *Neuroscience*, *334*, 39-46.

Geßner, C., Krüger, A., Folkow, L. P., Fehrle, W., Mikkelsen, B., & Burmester, T. (2022). Transcriptomes suggest that pinniped and cetacean brains have a high capacity for aerobic metabolism while reducing energy-intensive processes such as synaptic transmission. *Frontiers in Molecular Neuroscience*, *15*, 877349.

Hadzic, A., Nguyen, T. D., Hosoyamada, M., Tomioka, N. H., Bergersen, L. H., Storm-Mathisen, J., & Morland, C. (2020). The lactate receptor HCA1 is present in the choroid plexus, the tela choroidea, and the neuroepithelial lining of the dorsal part of the third ventricle. *International Journal of Molecular Sciences*, *21*(18), 6457.

Harris, J. J., Jolivet, R., & Attwell, D. (2012). Synaptic energy use and supply. *Neuron*, *75*(5), 762-777.

Heit, B. S., Dykas, P., Chu, A., Sane, A., & Larson, J. (2021). Synaptic and network contributions to anoxic depolarization in mouse hippocampal slices. *Neuroscience*, *461*, 102-117.

Henze, D. A., Borhegyi, Z., Csicsvari, J., Mamiya, A., Harris, K. D., & Buzsaki, G. (2000). Intracellular features predicted by extracellular recordings in the hippocampus in vivo. *Journal of neurophysiology*, *84*(1), 390-400.

Herrera-López, G., Griego, E., & Galván, E. J. (2020). Lactate induces synapse-specific potentiation on CA3 pyramidal cells of rat hippocampus. *PLoS One*, *15*(11), e0242309.

Hill, R. W., Wyse, G. A., & Anderson, M. (2018). Synapses. *Animal physiology. 4th ed. Sunderland: Sinauer Associates, Inc*, 337-368.

Hoff, M. L. M., Fabrizius, A., Czech-Damal, N. U., Folkow, L. P., & Burmester, T. (2017). Transcriptome analysis identifies key metabolic changes in the hooded seal (Cystophora cristata) brain in response to hypoxia and reoxygenation. *PLoS One*, *12*(1), e0169366.

Ikemoto, A., Bole, D. G., & Ueda, T. (2003). Glycolysis and glutamate accumulation into synaptic vesicles: Role of glyceraldehyde phosphate dehydrogenase and 3-phosphoglycerate kinase. *Journal of Biological Chemistry*, *278*(8), 5929-5940.

Ishida, A., Noda, Y., & Ueda, T. (2009). Synaptic vesicle-bound pyruvate kinase can support vesicular glutamate uptake. *Neurochemical research*, *34*, 807-818.

Izzo, L. T., & Wellen, K. E. (2019). Histone lactylation links metabolism and gene regulation.

Kasischke, K. A., Vishwasrao, H. D., Fisher, P. J., Zipfel, W. R., & Webb, W. W. (2004). Neural activity triggers neuronal oxidative metabolism followed by astrocytic glycolysis. *Science*, *305*(5680), 99-103.

Kerem, D., & Elsner, R. (1973). Cerebral tolerance to asphyxial hypoxia in the harbor seal. *Respiration physiology*, *19*(2), 188-200.

Knierim, J. J. (2015). The hippocampus. *Current Biology*, *25*(23), R1116-R1121.

Kooyman, G. L., Wahrenbrock, E. A., Castellini, M. A., Davis, R. W., & Sinnett, E. E. (1980). Evidence of preferred pathways from blood chemistry and behavior. *J. comp. Physiol*, *138*, 335-346.

Kooyman, G. L., Castellini, M. A., Davis, R. W., & Maue, R. A. (1983). Aerobic diving limits of immature Weddell seals. *Journal of Comparative Physiology*, *151*, 171-174.

Kovacs, K. M., & Lavigne, D. M. (1986). Cystophora cristata. *Mammalian Species*, (258), 1-9.

Lager, M. (2020). *Molecular and serological tools for clinical diagnostics of Lyme borreliosis-can the laboratory analysis be improved?* (Vol. 1744). Linköping University Electronic Press.

Lambertus, M., Øverberg, L. T., Andersson, K. A., Hjelden, M. S., Hadzic, A., Haugen, Ø. P., ... & Morland, C. (2021). L-lactate induces neurogenesis in the mouse ventricular-subventricular zone via the lactate receptor HCA1. *Acta Physiologica*, *231*(3), e13587.

Larson, J., & Park, T. J. (2009). Extreme hypoxia tolerance of naked mole-rat brain. *Neuroreport*, *20*(18), 1634-1637.

Larson, J., Drew, K. L., Folkow, L. P., Milton, S. L., & Park, T. J. (2014). No oxygen? No problem! Intrinsic brain tolerance to hypoxia in vertebrates. *Journal of Experimental Biology*, *217*(7), 1024-1039.

Lauritzen, K. H., Morland, C., Puchades, M., Holm-Hansen, S., Hagelin, E. M., Lauritzen, F., ... & Bergersen, L. H. (2014). Lactate receptor sites link neurotransmission, neurovascular coupling, and brain energy metabolism. *Cerebral cortex*, *24*(10), 2784-2795.

Lee, D. K., Nguyen, T., Lynch, K. R., Cheng, R., Vanti, W. B., Arkhitko, O., ... & O'Dowd, B. F. (2001). Discovery and mapping of ten novel G protein-coupled receptor genes. *Gene*, *275*(1), 83-91.

Lenfant, C., Johansen, K., & Torrance, J. D. (1970). Gas transport and oxygen storage capacity in some pinnipeds and the sea otter. *Respiration Physiology*, *9*(2), 277-286.

Lipton, P. E. T. E. R., & Whittingham, T. S. (1979). The effect of hypoxia on evoked potentials in the in vitro hippocampus. *The Journal of physiology*, *287*(1), 427-438.

Lipton, P. (1999). Ischemic cell death in brain neurons. *Physiological reviews*, *79*(4), 1431-1568.

Liu, C., Wu, J., Zhu, J., Kuei, C., Yu, J., Shelton, J., ... & Lovenberg, T. W. (2009). Lactate inhibits lipolysis in fat cells through activation of an orphan G-protein-coupled receptor, GPR81. *Journal of Biological Chemistry*, *284*(5), 2811-2822.

Ludvigsen, S. (2010). Neuronal hypoxia tolerance in diving endotherms.

Lutz, P. L., Nilsson, G. E., & Prentice, H. M. (2003). *The brain without oxygen: causes of failure-physiological and molecular mechanisms for survival*. Springer Science & Business Media.

Madden, D. R. (2002). The structure and function of glutamate receptor ion channels. *Nature Reviews Neuroscience*, *3*(2), 91-101.

Magistretti, P. J., & Allaman, I. (2018). Lactate in the brain: from metabolic end-product to signalling molecule. *Nature Reviews Neuroscience*, *19*(4), 235-249.

Mao, H., Elkin, B. S., Genthikatti, V. V., Morrison III, B., & Yang, K. H. (2013). Why is CA3 more vulnerable than CA1 in experimental models of controlled cortical impact-induced brain injury?. *Journal of neurotrauma*, *30*(17), 1521-1530.

Mathis, D. M., Furman, J. L., & Norris, C. M. (2011). Preparation of acute hippocampal slices from rats and transgenic mice for the study of synaptic alterations during aging and amyloid pathology. *JoVE (Journal of Visualized Experiments)*, (49), e2330.

Meir, J. U., Champagne, C. D., Costa, D. P., Williams, C. L., & Ponganis, P. J. (2009). Extreme hypoxemic tolerance and blood oxygen depletion in diving elephant seals. *American Journal of Physiology-Regulatory, Integrative and Comparative Physiology*, *297*(4), R927-R939.

Mink, J. W., Blumenschine, R. J., & Adams, D. B. (1981). Ratio of central nervous system to body metabolism in vertebrates: its constancy and functional basis. *American Journal of Physiology-Regulatory, Integrative and Comparative Physiology*, *241*(3), R203-R212.

Mitz, S. A., Reuss, S., Folkow, L. P., Blix, A. S., Ramirez, J. M., Hankeln, T., & Burmester, T. (2009). When the brain goes diving: glial oxidative metabolism may confer hypoxia tolerance to the seal brain. *Neuroscience*, *163*(2), 552-560.

Morland, C., Lauritzen, K. H., Puchades, M., Holm-Hansen, S., Andersson, K., Gjedde, A., ... & Bergersen, L. H. (2015). The lactate receptor, G-protein-coupled receptor 81/hydroxycarboxylic acid receptor 1: Expression and action in brain. *Journal of neuroscience research*, *93*(7), 1045-1055.

Morland, C., Andersson, K. A., Haugen, Ø. P., Hadzic, A., Kleppa, L., Gille, A., ... & Bergersen, L. H. (2017). Exercise induces cerebral VEGF and angiogenesis via the lactate receptor HCAR1. *Nature communications*, *8*(1), 15557.

Morris, A. A. M. (2005). Cerebral ketone body metabolism. *Journal of inherited metabolic disease*, *28*(2), 109-121.

Murphy, B., Zapol, W. M., & Hochachka, P. W. (1980). Metabolic activities of heart, lung, and brain during diving and recovery in the Weddell seal. *Journal of Applied Physiology*, *48*(4), 596-605.

Nezhady, M. A. M., & Chemtob, S. (2021). 3-OBA is not an antagonist of GPR81. *Frontiers in Pharmacology*, *12*.

Novelli, A., Reilly, J. A., Lysko, P. G., & Henneberry, R. C. (1988). Glutamate becomes neurotoxic via the N-methyl-D-aspartate receptor when intracellular energy levels are reduced. *Brain research*, *451*(1-2), 205-212.

Odden, A., Folkow, L. P., Caputa, M., Hotvedt, R., & Blix, A. S. (1999). Brain cooling in diving seals. *Acta physiologica scandinavica*, *166*(1), 77-78.

Offermanns, S. (2017). Hydroxy-carboxylic acid receptor actions in metabolism. *Trends in Endocrinology & Metabolism*, *28*(3), 227-236.

Pellerin, L., & Magistretti, P. J. (1994). Glutamate uptake into astrocytes stimulates aerobic glycolysis: a mechanism coupling neuronal activity to glucose utilization. *Proceedings of the National Academy of Sciences*, *91*(22), 10625-10629.

Pellerin, L., & Magistretti, P. J. (2012). Sweet sixteen for ANLS. *Journal of Cerebral Blood Flow & Metabolism*, *32*(7), 1152-1166.

Peterson, C. L., & Laniel, M. A. (2004). Histones and histone modifications. *Current Biology*, *14*(14), R546-R551.

Peterson, B. L., Larson, J., Buffenstein, R., Park, T. J., & Fall, C. P. (2012). Blunted neuronal calcium response to hypoxia in naked mole-rat hippocampus. *PloS one*, *7*(2), e31568.

Ramirez, J. M., Folkow, L. P., & Blix, A. S. (2007). Hypoxia tolerance in mammals and birds: from the wilderness to the clinic. *Annu. Rev. Physiol.*, *69*, 113-143.

Ramirez, J. M., Folkow, L. P., Ludvigsen, S., Ramirez, P. N., & Blix, A. S. (2011). Slow intrinsic oscillations in thick neocortical slices of hypoxia tolerant deep diving seals. *Neuroscience*, *177*, 35-42.

Rangaraju, V., Calloway, N., & Ryan, T. A. (2014). Activity-driven local ATP synthesis is required for synaptic function. *Cell*, *156*(4), 825-835.

Rolfe, D. F., & Brown, G. C. (1997). Cellular energy utilization and molecular origin of standard metabolic rate in mammals. *Physiological reviews*, *77*(3), 731-758.

Rudolphi, K. A., Schubert, P., Parkinson, F. E., & Fredholm, B. B. (1992). Neuroprotective role of adenosine in cerebral ischaemia. *Trends in pharmacological sciences*, *13*, 439-445.

Schneuer, M., Flachsbarth, S., Czech-Damal, N. U., Folkow, L. P., Siebert, U., & Burmester, T. (2012). Neuroglobin of seals and whales: evidence for a divergent role in the diving brain. *Neuroscience*, *223*, 35-44.

Scholander, P. F. (1940). *Experimental investigations on the respiratory function in diving mammals and birds* (No. 22). I kommisjon hos Jacob Dybwad.

Schulz, P. E., Cook, E. P., & Johnston, D. (1994). Changes in paired-pulse facilitation suggest presynaptic involvement in long-term potentiation. *Journal of Neuroscience*, *14*(9), 5325-5337.

Schurr, A., West, C. A., & Rigor, B. M. (1988). Lactate-supported synaptic function in the rat hippocampal slice preparation. *Science*, *240*(4857), 1326-1328.

Schurr, A. (2002). Lactate, glucose and energy metabolism in the ischemic brain. *International journal of molecular medicine*, *10*(2), 131-136.

Sebastiao, A. M., de Mendonca, A., Moreira, T., & Ribeiro, J. A. (2001). Activation of synaptic NMDA receptors by action potential-dependent release of transmitter during hypoxia impairs recovery of synaptic transmission on reoxygenation. *Journal of Neuroscience*, *21*(21), 8564-8571.

Skwarzynska, D., Sun, H., Williamson, J., Kasprzak, I., & Kapur, J. (2023). Glycolysis regulates neuronal excitability via lactate receptor, HCA1R. *Brain*, *146*(5), 1888-1902.

Snyder, G. K. (1983). Respiratory adaptations in diving mammals. *Respiration physiology*, *54*(3), 269-294.

Sokoloff, L. O. U. I. S. (1973). Metabolism of ketone bodies by the brain. *Annual review of medicine*, *24*(1), 271-280.

Szmant, H. H. (1975). Physical properties of dimethyl sulfoxide and its function in biological systems. *Ann NY Acad Sci*, *243*(1), 20-3.

Taylor, S. C., Nadeau, K., Abbasi, M., Lachance, C., Nguyen, M., & Fenrich, J. (2019). The ultimate qPCR experiment: producing publication quality, reproducible data the first time. *Trends in biotechnology*, *37*(7), 761-774.

Tsao, C. W., Aday, A. W., Almarzooq, Z. I., Anderson, C. A., Arora, P., Avery, C. L., ... & American Heart Association Council on Epidemiology and Prevention Statistics Committee and Stroke Statistics Subcommittee. (2023). Heart disease and stroke statistics—2023 update: a report from the American Heart Association. *Circulation*, *147*(8), e93-e621.

Turrens, J. F. (2003). Mitochondrial formation of reactive oxygen species. *The Journal of physiology*, *552*(2), 335-344.

Vacquie-Garcia, J., Lydersen, C., Biuw, M., Haug, T., Fedak, M. A., & Kovacs, K. M. (2017). Hooded seal Cystophora cristata foraging areas in the Northeast Atlantic Ocean—Investigated using three complementary methods. *PLoS One*, *12*(12), e0187889.

VanGuilder, H. D., Vrana, K. E., & Freeman, W. M. (2008). Twenty-five years of quantitative PCR for gene expression analysis. *Biotechniques*, *44*(5), 619-626.

Vistein, R., & Puthenveedu, M. A. (2013). Reprogramming of G protein-coupled receptor recycling and signaling by a kinase switch. *Proceedings of the National Academy of Sciences*, *110*(38), 15289-15294.

Weinberg, Z. Y., & Puthenveedu, M. A. (2019). Regulation of G protein-coupled receptor signaling by plasma membrane organization and endocytosis. *Traffic*, *20*(2), 121-129.

Wittenberg, B. A., & Wittenberg, J. B. (1989). Transport of oxygen in muscle. *Annual Review of Physiology*, *51*(1), 857-878.

Zhang, D., Tang, Z., Huang, H., Zhou, G., Cui, C., Weng, Y., ... & Zhao, Y. (2019). Metabolic regulation of gene expression by histone lactylation. *Nature*, *574*(7779), 575-580.

Zucker, R. S. (1989). Short-term synaptic plasticity. *Annual review of neuroscience*, *12*(1), 13-31.

Zucker, R. S., & Regehr, W. G. (2002). Short-term synaptic plasticity. *Annual review of physiology*, *64*(1), 355-405.

Appendixes

Appendix A: Stability of the reference genes for qPCR

Genes Geomean of ranking values
TBP 1.00
HPRT1 1.68
GAPDH 3.00
RPL13A 4.00
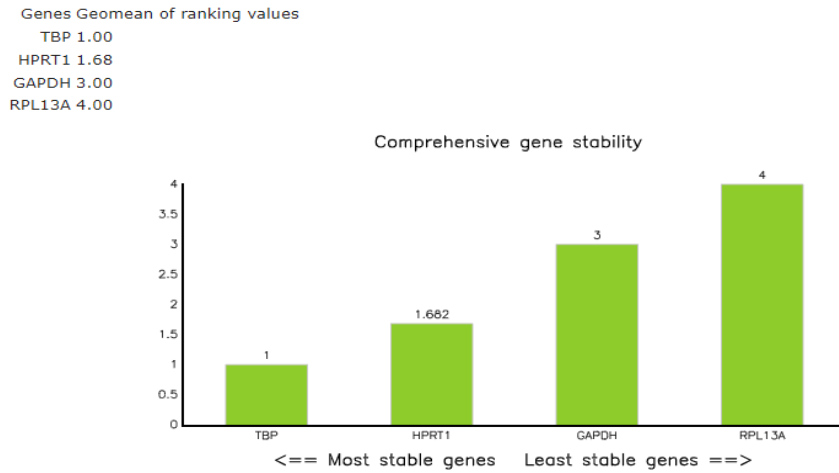
Figure A 1 Comprehensive gene stability of the reference genes.

Gene name   Stability value
HPRT1 | TBP 0.000
GAPDH   0.277
RPL13A   2.853
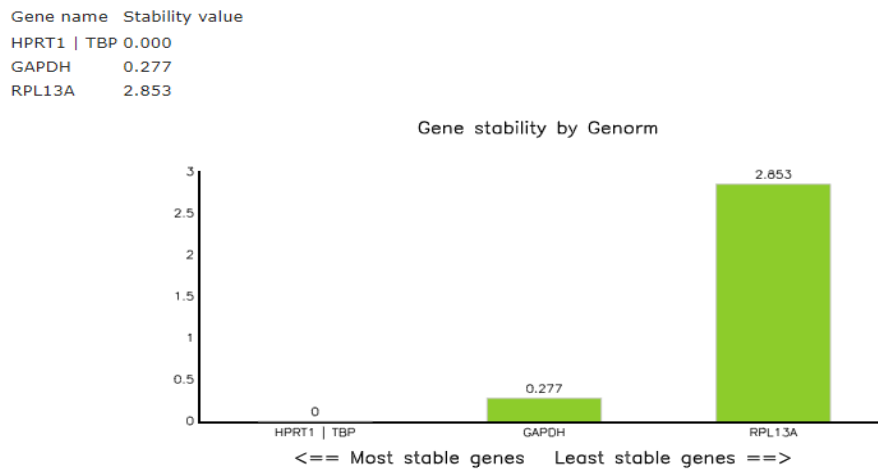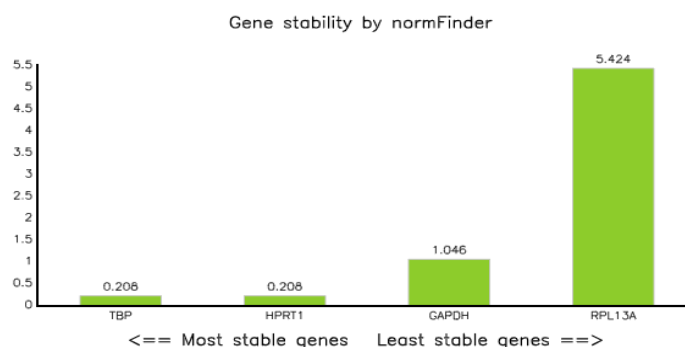
Figure A 2 Gene stability of the reference genes by Genorm.

Appendix B: Macros used for data extraction in LabChart

```
Sub FindAdd ()

      ' Move the insertion point to the beginning of the file
      Call Doc.SelectChannel(-1, True)
      Call Doc.SetSelectionTime(0, 0, 0, 0)

      Do While True


            ' Begin Find
            ChannelIndex = kCurrentChannel
            SetAction = kSetActivePoint
            SelectMode = kSelectBefore
            SelectTime = 0.001
            DataDisplayMode = kViewDataVisible
            SelectAll = False
            Direction = kSearchForward
            FindType = "Data above"
            FindData = "Limit=30;"
            Call Doc.Find (ChannelIndex, SetAction, SelectMode, SelectTime,
DataDisplayMode, SelectAll, Direction, FindType, FindData)
            ' End Find

            ' The function below will return true if the last operation failed, which
will cause the current loop to exit
            If (Services.ShouldExitCurrentRepeat()) Then Exit Do

            ' Begin Find
            ChannelIndex = kCurrentChannel
            SetAction = kSetPeriod
            SelectMode = kSelectBefore
            SelectTime = 0.001
            DataDisplayMode = kViewDataVisible
            SelectAll = False
            Direction = kSearchForward
            FindType = "Move backward"
            FindData = "AmountToMove=0.0002;"
            Call Doc.Find (ChannelIndex, SetAction, SelectMode, SelectTime,
DataDisplayMode, SelectAll, Direction, FindType, FindData)
            ' End Find
```

```
              ' The function below will return true if the last operation failed, which
will cause the current loop to exit
              If (Services.ShouldExitCurrentRepeat()) Then Exit Do

              Call Doc.AddToDataPad () 'baseline


              ' Begin Find
              ChannelIndex = kCurrentChannel
              SetAction = kSetActivePoint
              SelectMode = kSelectBefore
              SelectTime = 0.001
              DataDisplayMode = kViewDataVisible
              SelectAll = False
              Direction = kSearchForward
              FindType = "Move forward"
              FindData = "AmountToMove=0.002;"
              Call Doc.Find (ChannelIndex, SetAction, SelectMode, SelectTime,
DataDisplayMode, SelectAll, Direction, FindType, FindData)
              ' End Find


              ' Begin Find
              ChannelIndex = kCurrentChannel
              SetAction = kSetToPreviousPoint
              SelectMode = kSelectBefore
              SelectTime = 0.001
              DataDisplayMode = kViewDataVisible
              SelectAll = False
              Direction = kSearchForward
              FindType = "Move forward"
              FindData = "AmountToMove=0.007;"
              Call Doc.Find (ChannelIndex, SetAction, SelectMode, SelectTime,
DataDisplayMode, SelectAll, Direction, FindType, FindData)
              ' End Find

              Call Doc.AddToDataPad () ' Peak value

              ' The function below will return true if the last operation failed, which
will cause the current loop to exit
              If (Services.ShouldExitCurrentRepeat()) Then Exit Do
        Loop

End Sub
```

Appendix C: Tables from statistical analyses in GraphPad

Table A 1 *T-test, effect of lactate, seals compared to mice*

Table Analyzed	seal_vs_mouse
Column E	mouse_lactate
vs.	vs,
Column B	seal_lactate
Unpaired t test	
P value	0,0446
P value summary	*
Significantly different (P < 0.05)?	Yes
One- or two-tailed P value?	Two-tailed
t, df	t=2,242, df=12
How big is the difference?	
Mean of column B	78,33

Mean of column E	54,42
Difference between means (E - B) ± SEM	-23,91 ± 10,66
95% confidence interval	-47,15 to -0,6788
R squared (eta squared)	0,2953
F test to compare variances	
F, DFn, Dfd	10,75, 5, 7
P value	0,0070
P value summary	**
Significantly different (P < 0.05)?	Yes
Data analyzed	
Sample size, column B	8
Sample size, column E	6

Table A 2 *T-test, effect of rinsing after lactate, seals compared to mice*

Table Analyzed	**seal_vs_mouse**
Column F	mouse_rinse
vs.	vs,
Column C	seal_rinse
Unpaired t test	
P value	0,0042
P value summary	**
Significantly different (P < 0.05)?	Yes
One- or two-tailed P value?	Two-tailed
t, df	t=3,524, df=12
How big is the difference?	
Mean of column C	96,73
Mean of column F	67,07
Difference between means (F - C) ± SEM	-29,67 ± 8,417
95% confidence interval	-48,01 to -11,33
R squared (eta squared)	0,5086
F test to compare variances	
F, DFn, Dfd	3,879, 5, 7
P value	0,1056
P value summary	ns
Significantly different (P < 0.05)?	No
Data analyzed	
Sample size, column C	8
Sample size, column F	6

Table A 3 *T-test, effect of 3,5-DHBA (1mM), seals compared to mice*

Table Analyzed	**seal_vs_mouse**
Column G	1mM_mouse
vs.	vs,
Column B	1mM_seal
Unpaired t test	
P value	0,5559
P value summary	ns
Significantly different (P < 0.05)?	No
One- or two-tailed P value?	Two-tailed
t, df	t=0,6307, df=5
How big is the difference?	
Mean of column B	88,37

Mean of column G	92,56
Difference between means (G - B) ± SEM	4,182 ± 6,631
95% confidence interval	-12,86 to 21,23
R squared (eta squared)	0,07369
F test to compare variances	
F, DFn, Dfd	1,006, 3, 2
P value	
P value summary	
Significantly different (P < 0.05)?	No
Data analyzed	
Sample size, column B	4
Sample size, column G	3

Table A 4 *T-test, effect of 3,5-DHBA (2mM), seals compared to mice*

Table Analyzed	seal_vs_mouse
Column H	2mM_mouse
vs.	vs,
Column C	2mM_seal
Unpaired t test	
P value	0,1177
P value summary	ns
Significantly different (P < 0.05)?	No
One- or two-tailed P value?	Two-tailed
t, df	t=1,888, df=5
How big is the difference?	
Mean of column C	77,93
Mean of column H	93,04
Difference between means (H - C) ± SEM	15,11 ± 8,003
95% confidence interval	-5,466 to 35,68
R squared (eta squared)	0,4161
F test to compare variances	
F, DFn, Dfd	1,228, 2, 3
P value	0,8152
P value summary	ns
Significantly different (P < 0.05)?	No
Data analyzed	
Sample size, column C	4
Sample size, column H	3

Table A 5 *T-test, effect of 3,5-DHBA (4mM), seals compared to mice*

Table Analyzed	seal_vs_mouse
Column I	4mM_mouse
vs.	vs,
Column D	4mM_seal
Unpaired t test	
P value	0,1479
P value summary	ns
Significantly different (P < 0.05)?	No
One- or two-tailed P value?	Two-tailed
t, df	t=1,710, df=5
How big is the difference?	
Mean of column D	70,01

Mean of column I	81,85
Difference between means (I - D) ± SEM	11,83 ± 6,918
95% confidence interval	-5,952 to 29,61
R squared (eta squared)	0,3691
F test to compare variances	
F, DFn, Dfd	1,732, 2, 3
P value	0,6323
P value summary	ns
Significantly different (P < 0.05)?	No
Data analyzed	
Sample size, column D	4
Sample size, column I	3

Table A 6 *T-test, effect of 3,5-DHBA (rinse), seals compared to mice*

Table Analyzed	**seal_vs_mouse**
Column J	rinse_mouse
vs.	vs,
Column E	rinse_seal
Unpaired t test	
P value	0,7877
P value summary	ns
Significantly different (P < 0.05)?	No
One- or two-tailed P value?	Two-tailed
t, df	t=0,2841, df=5
How big is the difference?	
Mean of column E	107,0
Mean of column J	99,10
Difference between means (J - E) ± SEM	-7,941 ± 27,95
95% confidence interval	-79,79 to 63,91
R squared (eta squared)	0,01589
F test to compare variances	
F, DFn, Dfd	2,033, 3, 2
P value	0,6930
P value summary	ns
Significantly different (P < 0.05)?	No
Data analyzed	
Sample size, column E	4
Sample size, column J	3

Table A 7 *T-test, effect of 3Cl-HBA (40uM), seals compared to mice*

Table Analyzed	**seal_vs_mouse**
Column H	mouse_[40µM]
vs.	vs,
Column B	seal_[40µM]
Unpaired t test	
P value	0,1340
P value summary	ns
Significantly different (P < 0.05)?	No
One- or two-tailed P value?	Two-tailed
t, df	t=1,787, df=5
How big is the difference?	
Mean of column B	96,67

Mean of column H	106,9
Difference between means (H - B) ± SEM	10,22 ± 5,719
95% confidence interval	-4,482 to 24,92
R squared (eta squared)	0,3897
F test to compare variances	
F, DFn, Dfd	4,068, 2, 3
P value	0,2797
P value summary	ns
Significantly different (P < 0.05)?	No
Data analyzed	
Sample size, column B	4
Sample size, column H	3

Table A 8 T-test, effect of 3Cl-HBA (48uM), seals compared to mice

Table Analyzed	**seal_vs_mouse**
Column I	mouse_[80µM]
vs.	vs,
Column C	seal_[80µM]
Unpaired t test	
P value	0,9113
P value summary	ns
Significantly different (P < 0.05)?	No
One- or two-tailed P value?	Two-tailed
t, df	t=0,1171, df=5
How big is the difference?	
Mean of column C	92,93
Mean of column I	91,45
Difference between means (I - C) ± SEM	-1,479 ± 12,62
95% confidence interval	-33,93 to 30,97
R squared (eta squared)	0,002737
F test to compare variances	
F, DFn, Dfd	12,33, 2, 3
P value	0,0714
P value summary	ns
Significantly different (P < 0.05)?	No
Data analyzed	
Sample size, column C	4
Sample size, column I	3

Table A 9 T-test, effect of 3Cl-HBA (160uM), seals compared to mice

Table Analyzed	**seal_vs_mouse**
Column J	mouse_[160µM]
vs.	vs,
Column D	seal_[160µM]
Unpaired t test	
P value	0,4027
P value summary	ns
Significantly different (P < 0.05)?	No
One- or two-tailed P value?	Two-tailed
t, df	t=0,9138, df=5
How big is the difference?	
Mean of column D	94,39
Mean of column J	78,69

Difference between means (J - D) ± SEM	-15,69 ± 17,17
95% confidence interval	-59,83 to 28,45
R squared (eta squared)	0,1431
F test to compare variances	
F, DFn, Dfd	12,99, 2, 3
P value	0,0666
P value summary	ns
Significantly different (P < 0.05)?	No
Data analyzed	
Sample size, column D	4
Sample size, column J	3

Table A 10 T-test, effect of 3Cl-HBA (320uM), seals compared to mice

Table Analyzed	**seal_vs_mouse**
Column K	mouse_[320µM]
vs.	vs,
Column E	seal_[320µM]
Unpaired t test	
P value	0,4380
P value summary	ns
Significantly different (P < 0.05)?	No
One- or two-tailed P value?	Two-tailed
t, df	t=0,8424, df=5
How big is the difference?	
Mean of column E	93,23
Mean of column K	76,38
Difference between means (K - E) ± SEM	-16,86 ± 20,01
95% confidence interval	-68,29 to 34,58
R squared (eta squared)	0,1243
F test to compare variances	
F, DFn, Dfd	7,109, 2, 3
P value	0,1455
P value summary	ns
Significantly different (P < 0.05)?	No
Data analyzed	
Sample size, column E	4
Sample size, column K	3

Table A 11 T-test, effect of 3Cl-HBA (rinse), seals compared to mice

Table Analyzed	**seal_vs_mouse**
Column L	mouse_Rinse
vs.	vs,
Column F	seal_Rinse
Unpaired t test	
P value	0,4404
P value summary	ns
Significantly different (P < 0.05)?	No
One- or two-tailed P value?	Two-tailed
t, df	t=0,8377, df=5
How big is the difference?	
Mean of column F	84,96
Mean of column L	66,00

Difference between means (L - F) ± SEM	-18,96 ± 22,63
95% confidence interval	-77,14 to 39,22
R squared (eta squared)	0,1231
F test to compare variances	
F, DFn, Dfd	3,253, 3, 2
P value	0,4879
P value summary	ns
Significantly different (P < 0.05)?	No
Data analyzed	
Sample size, column F	4
Sample size, column L	3

Table A 12 *Tukey's multiple comparisons test, lactate experiment on seals*

Number of families	1							
Number of comparisons per family	3							
Alpha	0,05							
Tukey's multiple comparisons test	Mean Diff,	95,00% CI of diff,	Below threshold?	Summary	Adjusted P Value			
Baseline vs. Lactate [20mM]	21,67	4,815 to 38,53	Yes	*	0,0146	A-B		
Baseline vs. Rinse	3,267	-13,59 to 20,12	No	ns	0,8534	A-C		
Lactate [20mM] vs. Rinse	-18,4	-35,26 to -1,548	Yes	*	0,0335	B-C		
Test details	Mean 1	Mean 2	Mean Diff,	SE of diff,	n1	n2	q	DF
Baseline vs. Lactate [20mM]	100	78,33	21,67	6,037	4	4	5,076	9
Baseline vs. Rinse	100	96,73	3,267	6,037	4	4	0,7654	9
Lactate [20mM] vs. Rinse	78,33	96,73	-18,4	6,037	4	4	4,311	9

Table A 13 *Tukey's multiple comparisons test, lactate experiment on mice*

Number of families	1			
Number of comparisons per family	3			
Alpha	0,05			
Tukey's multiple comparisons test	Mean Diff,	95,00% CI of diff,	Below threshold?	Summary
Baseline vs. Lactate [20mM]	45,58	-11,73 to 102,9	No	ns
Baseline vs. Rinse	32,93	-24,38 to 90,25	No	ns
Lactate [20mM] vs. Rinse	-12,65	-69,97 to 44,67	No	ns
Test details	Mean 1	Mean 2	Mean Diff,	SE of diff,
Baseline vs. Lactate [20mM]	100	54,42	45,58	18,68
Baseline vs. Rinse	100	67,07	32,93	18,68
Lactate [20mM] vs. Rinse	54,42	67,07	-12,65	18,68

Table A 14 *Tukey's multiple comparisons test, 3,5-DHBA experiment on seals*

Number of families	1			
Number of comparisons per family	10			
Alpha	0,05			
Tukey's multiple comparisons test	Mean Diff,	95,00% CI of diff,	Below threshold?	Summary
Baseline vs. 1mM	11,63	-11,43 to 34,68	No	ns
Baseline vs. 2mM	22,07	-4,532 to 48,67	No	ns
Baseline vs. 4mM	29,99	8,858 to 51,11	Yes	*
Baseline vs. Rinse	-7,042	-115,8 to 101,7	No	ns
1mM vs. 2mM	10,44	-9,267 to 30,15	No	ns
1mM vs. 4mM	18,36	5,462 to 31,26	Yes	*
1mM vs. Rinse	-18,67	-135,9 to 98,61	No	ns
2mM vs. 4mM	7,916	-4,882 to 20,71	No	ns
2mM vs. Rinse	-29,11	-144,2 to 86,02	No	ns
4mM vs. Rinse	-37,03	-144,6 to 70,57	No	ns
Test details	Mean 1	Mean 2	Mean Diff,	SE of diff,
Baseline vs. 1mM	100	88,37	11,63	4,346
Baseline vs. 2mM	100	77,93	22,07	5,015
Baseline vs. 4mM	100	70,01	29,99	3,983
Baseline vs. Rinse	100	107	-7,042	20,5
1mM vs. 2mM	88,37	77,93	10,44	3,716
1mM vs. 4mM	88,37	70,01	18,36	2,431
1mM vs. Rinse	88,37	107	-18,67	22,11
2mM vs. 4mM	77,93	70,01	7,916	2,413
2mM vs. Rinse	77,93	107	-29,11	21,7
4mM vs. Rinse	70,01	107	-37,03	20,28

X

Table A 15 *Tukey's multiple comparisons test, 3,5-DHBA experiment on mice*

Number of families	1			
Number of comparisons per family	15			
Alpha	0,05			
Tukey's multiple comparisons test	Mean Diff,	95,00% CI of diff,	Below threshold?	Summary
Baseline vs. 1mM	7,444	-34,07 to 48,96	No	ns
Baseline vs. 2mM	6,963	-46,29 to 60,21	No	ns
Baseline vs. 4mM	18,15	-32,06 to 68,37	No	ns
Baseline vs. 8mM	38,36	-28,43 to 105,2	No	ns
Baseline vs. Rinse	0,8991	-136,8 to 138,6	No	ns
1mM vs. 2mM	-0,4813	-29,71 to 28,75	No	ns
1mM vs. 4mM	10,71	0,6613 to 20,76	Yes	*
1mM vs. 8mM	30,92	5,007 to 56,83	Yes	*
1mM vs. Rinse	-6,545	-161,4 to 148,4	No	ns
2mM vs. 4mM	11,19	-12,95 to 35,33	No	ns
2mM vs. 8mM	31,4	-10,90 to 73,69	No	ns
2mM vs. Rinse	-6,064	-187,8 to 175,7	No	ns
4mM vs. 8mM	20,21	-0,6087 to 41,02	No	ns
4mM vs. Rinse	-17,26	-181,3 to 146,8	No	ns
8mM vs. Rinse	-37,46	-201,2 to 126,3	No	ns
Test details	Mean 1	Mean 2	Mean Diff,	SE of diff,
Baseline vs. 1mM	100	92,56	7,444	5,004
Baseline vs. 2mM	100	93,04	6,963	6,418
Baseline vs. 4mM	100	81,85	18,15	6,053
Baseline vs. 8mM	100	61,64	38,36	8,051
Baseline vs. Rinse	100	99,1	0,8991	16,6
1mM vs. 2mM	92,56	93,04	-0,4813	3,523
1mM vs. 4mM	92,56	81,85	10,71	1,211
1mM vs. 8mM	92,56	61,64	30,92	3,123
1mM vs. Rinse	92,56	99,1	-6,545	18,67
2mM vs. 4mM	93,04	81,85	11,19	2,909
2mM vs. 8mM	93,04	61,64	31,4	5,098
2mM vs. Rinse	93,04	99,1	-6,064	21,9
4mM vs. 8mM	81,85	61,64	20,21	2,509
4mM vs. Rinse	81,85	99,1	-17,26	19,77
8mM vs. Rinse	61,64	99,1	-37,46	19,74

Table A 16 *Tukey's multiple comparisons test, 3,5-DHBA, CA3 experiment on mice*

Number of families	1			
Number of comparisons per family	10			
Alpha	0,05			
Tukey's multiple comparisons test	Mean Diff,	95,00% CI of diff,	Below threshold?	Summary
Baseline vs. [1mM]	4,463	-59,29 to 68,22	No	ns
Baseline vs. [2mM]	-4,556	-32,78 to 23,67	No	ns
Baseline vs. [4mM]	-5,198	-77,56 to 67,17	No	ns
Baseline vs. Rinse	-32,91	-161,4 to 95,60	No	ns
[1mM] vs. [2mM]	-9,019	-58,81 to 40,78	No	ns
[1mM] vs. [4mM]	-9,662	-44,18 to 24,86	No	ns
[1mM] vs. Rinse	-37,38	-133,0 to 58,23	No	ns
[2mM] vs. [4mM]	-0,6424	-72,18 to 70,90	No	ns
[2mM] vs. Rinse	-28,36	-128,7 to 71,97	No	ns
[4mM] vs. Rinse	-27,72	-156,9 to 101,5	No	ns
Test details	Mean 1	Mean 2	Mean Diff,	SE of diff,
Baseline vs. [1mM]	100	95,54	4,463	8,286
Baseline vs. [2mM]	100	104,6	-4,556	3,669
Baseline vs. [4mM]	100	105,2	-5,198	9,405
Baseline vs. Rinse	100	132,9	-32,91	16,7
[1mM] vs. [2mM]	95,54	104,6	-9,019	6,472
[1mM] vs. [4mM]	95,54	105,2	-9,662	4,486
[1mM] vs. Rinse	95,54	132,9	-37,38	12,43
[2mM] vs. [4mM]	104,6	105,2	-0,6424	9,298
[2mM] vs. Rinse	104,6	132,9	-28,36	13,04
[4mM] vs. Rinse	105,2	132,9	-27,72	16,79

Table A 17 *Tukey's multiple comparisons test, 3Cl-HBA experiment on seals*

Number of families	1			
Number of comparisons per family	15			
Alpha	0,05			
Tukey's multiple comparisons test	Mean Diff,	95,00% CI of diff,	Below threshold?	Summary
Baseline vs. [40µM]	3,329	-10,93 to 17,59	No	ns
Baseline vs. [80µM]	7,071	-12,90 to 27,04	No	ns
Baseline vs. [160µM]	5,614	-20,92 to 32,15	No	ns
Baseline vs. [320µM]	6,769	-33,35 to 46,88	No	ns
Baseline vs. Rinse	15,04	-83,99 to 114,1	No	ns
[40µM] vs. [80µM]	3,742	-28,49 to 35,97	No	ns
[40µM] vs. [160µM]	2,285	-25,74 to 30,31	No	ns
[40µM] vs. [320µM]	3,44	-33,90 to 40,78	No	ns
[40µM] vs. Rinse	11,71	-83,51 to 106,9	No	ns
[80µM] vs. [160µM]	-1,457	-26,81 to 23,90	No	ns
[80µM] vs. [320µM]	-0,3018	-42,45 to 41,85	No	ns
[80µM] vs. Rinse	7,969	-89,47 to 105,4	No	ns
[160µM] vs. [320µM]	1,155	-16,51 to 18,82	No	ns
[160µM] vs. Rinse	9,425	-64,87 to 83,72	No	ns
[320µM] vs. Rinse	8,27	-50,69 to 67,23	No	ns
Test details	Mean 1	Mean 2	Mean Diff,	SE of diff,
Baseline vs. [40µM]	100	96,67	3,329	2,509
Baseline vs. [80µM]	100	92,93	7,071	3,514
Baseline vs. [160µM]	100	94,39	5,614	4,669
Baseline vs. [320µM]	100	93,23	6,769	7,059
Baseline vs. Rinse	100	84,96	15,04	17,43
[40µM] vs. [80µM]	96,67	92,93	3,742	5,671
[40µM] vs. [160µM]	96,67	94,39	2,285	4,931
[40µM] vs. [320µM]	96,67	93,23	3,44	6,57
[40µM] vs. Rinse	96,67	84,96	11,71	16,76
[80µM] vs. [160µM]	92,93	94,39	-1,457	4,462
[80µM] vs. [320µM]	92,93	93,23	-0,3018	7,416
[80µM] vs. Rinse	92,93	84,96	7,969	17,14
[160µM] vs. [320µM]	94,39	93,23	1,155	3,108
[160µM] vs. Rinse	94,39	84,96	9,425	13,07
[320µM] vs. Rinse	93,23	84,96	8,27	10,37

Table A 18 *Tukey's multiple comparisons test, 3Cl-HBA experiment on mouse*

Number of families	1		
Number of comparisons per family	15		
Alpha	0,05		
Tukey's multiple comparisons test	Mean Diff,	95,00% CI of diff,	Below threshold?
Baseline vs. [40µM]	-6,889	-55,36 to 41,58	No
Baseline vs. [80µM]	8,55	-109,7 to 126,8	No
Baseline vs. [160µM]	21,31	-139,9 to 182,5	No
Baseline vs. [320µM]	23,62	-156,7 to 203,9	No
Baseline vs. Rinse	34	-58,56 to 126,6	No
[40µM] vs. [80µM]	15,44	-140,4 to 171,3	No
[40µM] vs. [160µM]	28,2	-168,7 to 225,1	No
[40µM] vs. [320µM]	30,51	-190,7 to 251,7	No
[40µM] vs. Rinse	40,89	-100,0 to 181,8	No
[80µM] vs. [160µM]	12,76	-30,62 to 56,13	No
[80µM] vs. [320µM]	15,07	-51,58 to 81,73	No
[80µM] vs. Rinse	25,45	-52,19 to 103,1	No
[160µM] vs. [320µM]	2,318	-37,54 to 42,17	No
[160µM] vs. Rinse	12,69	-100,6 to 126,0	No
[320µM] vs. Rinse	10,37	-101,9 to 122,7	No
Test details	Mean 1	Mean 2	Mean Diff,
Baseline vs. [40µM]	100	106,9	-6,889
Baseline vs. [80µM]	100	91,45	8,55
Baseline vs. [160µM]	100	78,69	21,31
Baseline vs. [320µM]	100	76,38	23,62
Baseline vs. Rinse	100	66	34
[40µM] vs. [80µM]	106,9	91,45	15,44
[40µM] vs. [160µM]	106,9	78,69	28,2
[40µM] vs. [320µM]	106,9	76,38	30,51
[40µM] vs. Rinse	106,9	66	40,89
[80µM] vs. [160µM]	91,45	78,69	12,76
[80µM] vs. [320µM]	91,45	76,38	15,07
[80µM] vs. Rinse	91,45	66	25,45
[160µM] vs. [320µM]	78,69	76,38	2,318
[160µM] vs. Rinse	78,69	66	12,69
[320µM] vs. Rinse	76,38	66	10,37